

LIGNIN AS A BIO-BASED ALTERNATIVE FOR PETROLEUM-DERIVED POLYOLS IN
FLEXIBLE POLYURETHANE FOAMS

By

Kevin Dunne

A THESIS

Submitted to
Michigan State University
in partial fulfillment of the requirements
for the degree of

Materials Science and Engineering – Master of Science

2024

ABSTRACT

In recent years, there have been extensive efforts to replace fossil-fuel-based raw materials with bio-based materials in flexible polyurethane (PU) foams. Lignin, a natural polyol generated as a byproduct of chemical pulping and biorefineries, is an attractive compound to replace petroleum-derived polyols due to its abundant availability and bio-based nature. This thesis discusses efforts to partially replace petrochemical polyols in flexible foams with a liquid lignin polyol made by oxyalkylating lignin with propylene carbonate, a green solvent. First, a small-scale computational study using density functional theory (DFT) was used to investigate the reaction between lignin model compounds and isocyanates. The results of this computational study were consistent with experimentally obtained data. Next, a screening study was conducted to determine how different types of lignin affect the properties of the developed lignin polyols. Then, flexible PU foams were made using three different lignin polyols, derived from different biomass sources and isolation processes. Electron microscopy and reaction profile analysis of foam samples showed that the addition of the lignin polyol reduced cell sizes and decreased reaction times. It was found that a high molecular weight kraft-softwood lignin resulted in a foam with significantly better mechanical properties compared to foams made with organosolv wheat straw and acid-hydrolysis hardwood lignins. After optimization, a foam produced containing 14% kraft-softwood lignin polyol met standard requirements for automotive seating applications.

Copyright by
KEVIN DUNNE
2024

ACKNOWLEDGEMENTS

It feels nearly impossible to fully express my gratitude for Dr. Mojgan Nejad, my advisor. I started in Dr. Nejad's lab 5 years ago as a freshman, and she has gone out of her way to provide me with life changing opportunities and mentorship. I especially appreciate her for encouraging me to think differently about problems and for giving me new challenges.

My committee members, Dr. Chris Saffron (Biomedical Engineering), Dr. Ramani Narayan, and Dr. Caroline Szczepanski have been very helpful regarding my project, and have given me new insights about my problem solving approach. I really appreciate the time and effort they have expended towards the completion of my master's thesis.

I also want to thank all of my lab-mates for their technical assistance and friendship. Saeid Nikafshar, who mentored me as an undergraduate, and Akash Gondaliya, who first introduced me to the topic of flexible polyurethane foams, were especially critical to the success of this project. I also worked very closely with Enoch Kofi Acquah and I would not have made much progress if it weren't for his help, guidance, and humorous encouragement. Furthermore, Kory McIntosh, Dr. Ed Drown of the Composite Materials and Structures Center, Dr. Daniel Holmes of the MSU NMR facility, and the staff at the Center for Advanced Microscopy provided invaluable assistance with instrumentation.

Lastly, I would like to thank my family. My parents have worked tirelessly to ensure that my brothers and I succeed inside and outside of the classroom, and they deserve all the credit for our success.

TABLE OF CONTENTS

LIST OF ABBREVIATIONS.....	vi
CHAPTER 1 Introduction.....	1
CHAPTER 2 Materials and Methods.....	19
CHAPTER 3 Results and Discussion	36
CHAPTER 4 Conclusions and Future Work	65
BIBLIOGRAPHY.....	71
APPENDIX.....	82

LIST OF ABBREVIATIONS

Polyurethane: PU

PC: Propylene Carbonate

pphp: parts per hundred polyol

DBU: 1,8-Diazabicyclo(5.4.0)undec-7-ene

NCO: Isocyanate group

OH: Hydroxy group

³¹P-NMR: Phosphorous-31 Nuclear Magnetic Resonance Spectroscopy

FTIR: Fourier Transform Infrared Spectroscopy

LP: Lignin-Polyol

O-WS: Organosolv Wheat Straw Lignin

K-SW: Kraft Softwood Lignin

H-HW: Acid-Hydrolysis Hardwood Lignin

SEM: Scanning Electron Microscopy

CFD: Compression Force Deflection

DMA: Dynamic Mechanical Analysis

DFT: Density Functional Theory

LM: Lignin Model Compound

CHAPTER 1 Introduction

1.1 Polyurethane Foams

Polyurethanes (PU) are a broad class of polymers used in a wide variety of applications, including adhesives, coatings, sealants, elastomers, and foams. PUs are typically formed from a condensation reaction between polyols and diisocyanates (Figure 1). However, many PU materials may also contain urea linkages formed as a side product of the reaction between water and isocyanates, which also generates carbon dioxide gas (Figure 2).^{1,2}

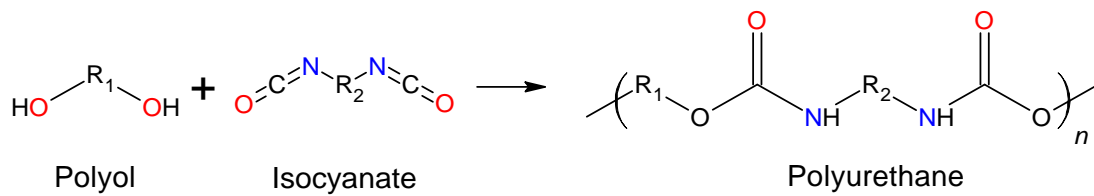


Figure 1. Urethane formation reaction

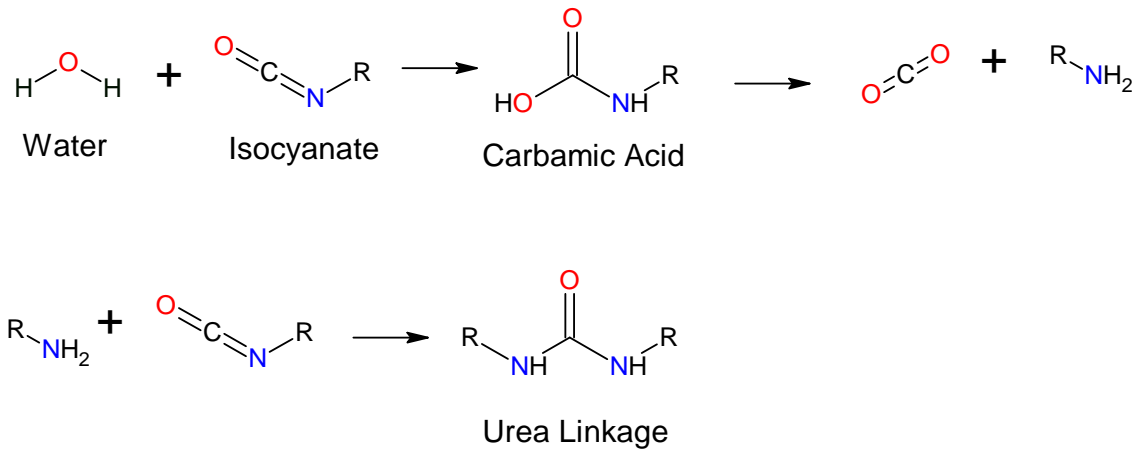


Figure 2. Generation of carbon dioxide and polyurea via the water-isocyanate reaction

A unique feature of PUs is their two phase, microphase separated structure. The long, low-polarity, and flexible chains of the polyol, termed the “soft segment” (SS) have low miscibility with the “hard segment” (HS) consisting of rigid, highly polar urethane and urea bonds and the aromatic isocyanate backbone. In accordance with Flory-Huggins solution theory,³ this causes PUs to undergo microphase separation, with the soft segment providing elastomeric

properties, while the hard segment provides both chemical and physical crosslinking that increase the strength of the foams.⁴ This unique morphology, which can be altered by the choice of raw materials, allows PUs to have unique and highly tunable mechanical properties.^{5,6}

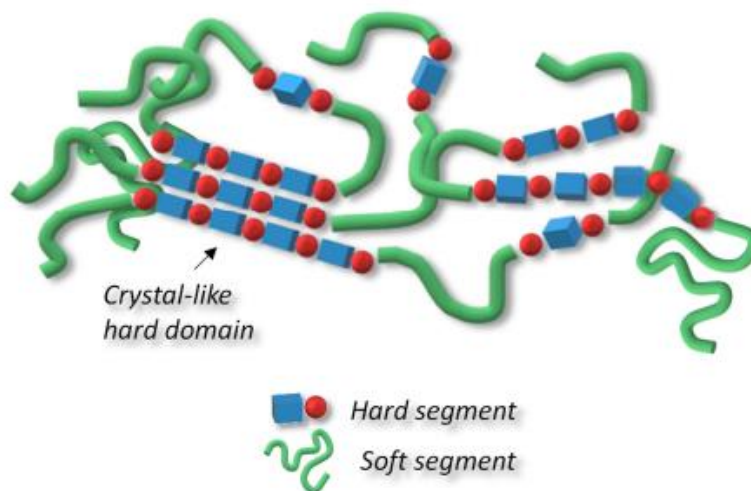


Figure 3. Schematic of hard and soft domains in PUs. Reproduced from⁴

PU foams are made by either physically blowing a gas into a foam as it cures, or by using a chemical reaction to generate gas while the foam cures.^{1,2} Water is commonly used as a chemical blowing agent as it reacts with isocyanate to produce carbon dioxide gas; however, water also increases the amount of urea linkages within the foam. A wide variety of catalysts, crosslinkers, and surfactants are used to tune the morphology and properties of the blown foams. PU foams are further divided into 3 major categories: rigid, semirigid, and flexible foams. Rigid foams are typically manufactured with high functionality, low molecular weight polyols, while flexible foams are typically made with high molecular weight, low functionality polyols ($f = 2-3$) that results in a much lower crosslinking density. The long, flexible polyol backbone is typically constructed from a polyether polyol derived synthesized from ethylene oxide and propylene oxide which are highly reactive, volatile, and carcinogenic raw materials.^{1,7,8} Typically, Toluene Diisocyanate (TDI) is used as the isocyanate in flexible foams, but in recent

years, polymeric methylene diphenyl diisocyanates (pMDI) have become an attractive alternative for flexible foam formulations because pMDI has a comparatively lower vapor pressure and toxicity.

Microstructurally, rigid foams have a high closed cell content, while flexible PU foams have an open-celled structure where gases can flow into and out of cells between struts of a polymer matrix.⁶ The flexible nature of these foams is derived from the elastic deformation of these struts. Flexible PU foams are one of the earliest and most important applications of PUs. In 2022, the total market volume of all PU materials was valued at 25 million metric tons per year, corresponding to a market value of 67 billion USD, and is expected to grow to 31 metric tons per year by 2030.^{9,10} In 2016, flexible foams comprised 31% of all PU products.¹¹ Because flexible PU foams are typically manufactured using petroleum-derived polyols and isocyanates, there is great interest in developing inexpensive, and sustainable raw materials for PUs.¹¹⁻¹³ Some examples of sustainable polyols include polycarbonate polyols synthesized using carbon dioxide¹⁴ and bio-based polyols synthesized from vegetable oils, such as soybean, linseed, and castor oil.^{15,16} A preliminary lifecycle analysis of Cargill's soybean based BiOH polyols, which has already been commercialized, resulted in 36% less global warming emissions and 61% less non-renewable energy use compared to their traditionally petroleum-derived polyols, demonstrating the.¹⁷ In 2022, the market for green and bio-based polyols was worth 4.6 billion USD, and is expected to grow to 9.3 billion by 2030.¹⁸ As a result, there is large motivation for developing sustainable polyols using new bio-based feedstocks and sustainable technologies.

1.2 Lignin

1.2.1 Lignin Sources

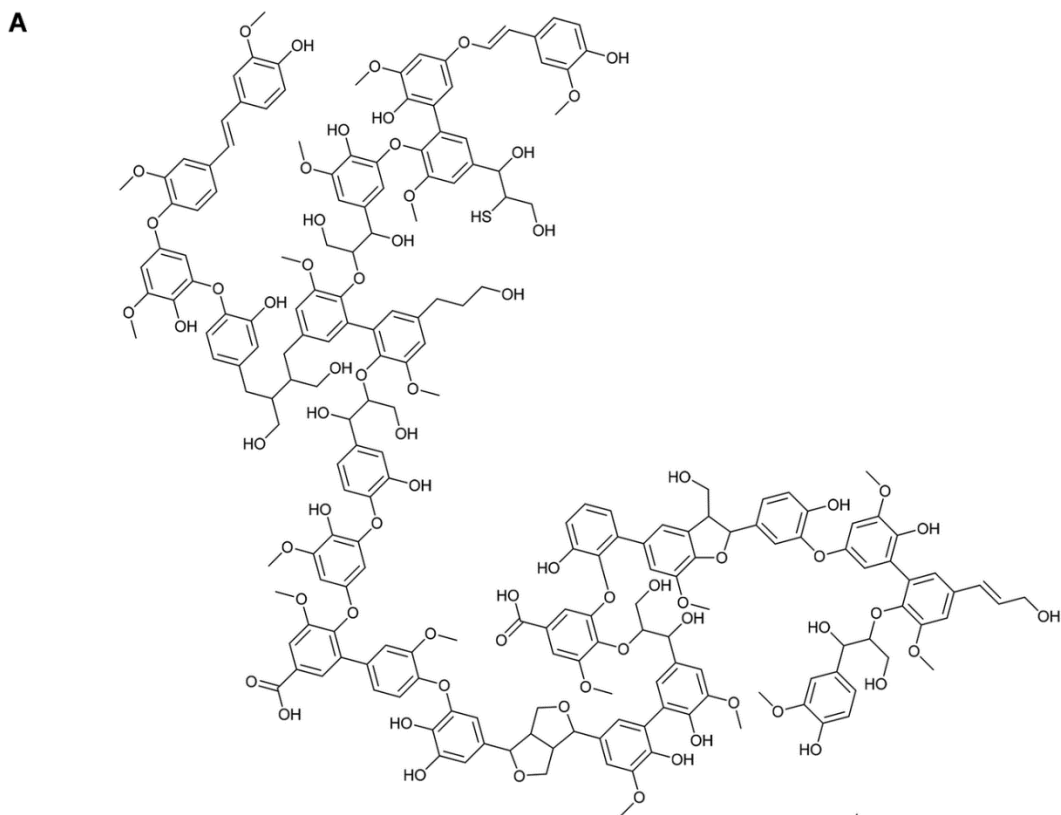


Figure 4. Structure of kraft-softwood lignin. Reproduced from Crestini et al.¹⁹

Lignin is the second most abundant naturally occurring polymer, after cellulose, and comprises up to 30% of dry mass of all biomass.²⁰ Acting as a binding matrix material in the cell walls of plants, lignin is an amorphous, highly crosslinked polymer derived from radical coupling of three phenylpropane units: *p*-coumaryl alcohol, coniferyl alcohol, and sinapyl alcohol, which respectively have 0, 1 and 2 methoxy groups at the ortho positions of the phenyl ring. These respectively form *p*-hydroxyphenyl (H), guaiacyl (G), and syringyl (S) structures in lignin. Lignins also contain a large amount of aliphatic hydroxyl groups, and a small amount of carboxylic acids. The type of biomass significantly affects the chemical structure of lignin.

Herbaceous plants contain all three types of lignin units, hardwood lignin comprises primarily G and S units, and softwood lignins are dominated by G units (Fig. 5).²¹

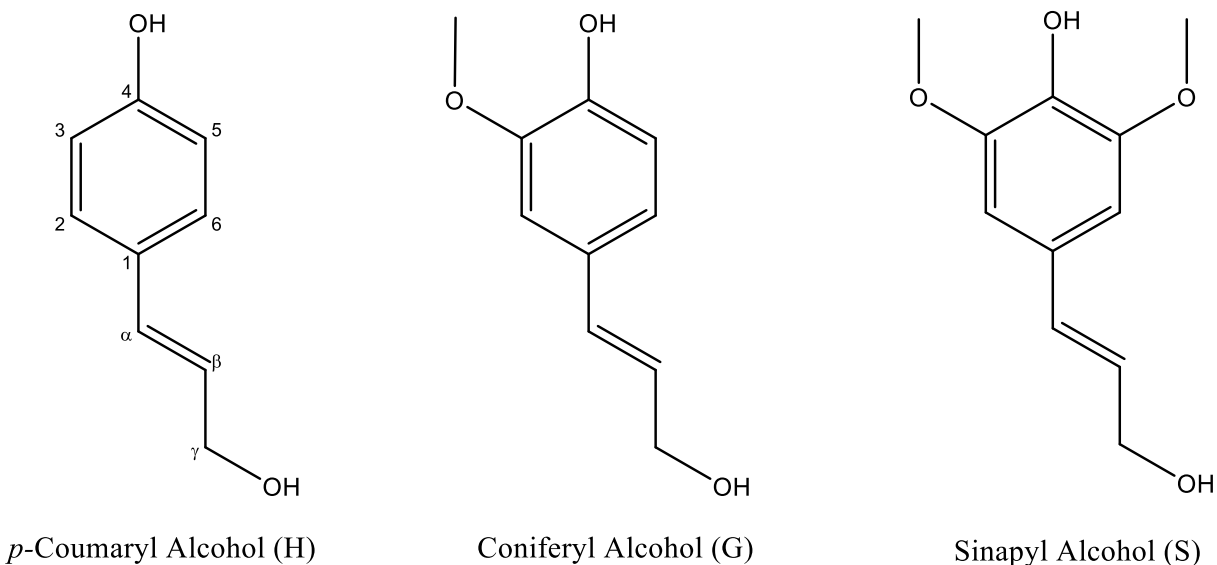


Figure 5. The three monolignols

1.2.2 Lignin Isolation Processes

Lignin is typically generated as a byproduct of pulping and biorefinery processes. The biomass source and isolation processes used to separate lignin from other plant biomass components (cellulose and hemicellulose) can significantly change lignin's chemical structure and properties. There are several major lignin isolation processes, including sulfite cooking, soda, kraft, kraft, hydrolysis, and organosolv. In sulfite cooking, aqueous sulfite salts (with a variety of cations including sodium, calcium, potassium, magnesium, and ammonium cations), are used at high temperatures to cleave bonds between lignin molecules and carbohydrates, as well as functionalizing lignin with sulfonate groups that make the water-soluble liginosulfonate.

Soda lignin is commonly produced by reacting herbaceous fibrous biomass in a sodium hydroxide solution at moderate temperatures. This process separates lignin from carbohydrates, but also cleaves aryl ether linkages resulting in an increase the number of hydroxyl groups in

lignin.^{22,23} The kraft process, which is widely used for processing woody biomass into wood pulp, has some similarities to the soda process, but uses both sodium hydroxide and sodium sulfide aqueous solutions to digest biomass around 170 °C.^{19,24} Both soda and kraft pulping processes also initiate a series of reactions resulting in the formation of condensed structures between lignin molecules, which can somewhat offset the fragmentation process. In both the kraft and soda processes, the removed lignin is contained in a crude alkaline solution called black liquor, which is typically combusted to produce energy for the pulping plant. Precipitation in acidic media can be used to extract the lignin from the black liquor. However, it should be noted that the kraft and soda processes promote repolymerization of lignin chains, increasing molecular weight.²⁵ Around 90% of pulping processes involve the kraft process, with the annual global production of technical kraft lignin being 265,000 tons/year in 2018, and has been forecast to reach up to 2,500,000 tons/year in 2025;²⁶ thus, there is great incentive to valorize the vast quantities of kraft lignin.

Hydrolysis is another method for processing biomass, but is more focused on breaking down carbohydrates into smaller sugars that can be used in other parts of the biorefinery, such as producing ethanol and nano- or microcrystalline celluloses. To produce lignin through lignocellulosic hydrolysis, the biomass is first “pretreated” by mechanical, thermal or chemical means; for instance, steam explosion of biomass makes it easier to process, solubilizes hemicellulose, and begins breaking down bonds connecting lignin and cellulose. Then, enzymes or inorganic acids in aqueous solutions can be used to catalyze the hydrolysis of cellulose into monosaccharides; simultaneously, some cleavage of some aryl-ether linkages in lignin occurs, increasing phenolic hydroxyl content and reducing molecular weight.^{27,28} Lignin, which is left as a residue, can be extracted by acid precipitation or in a dioxane-water solution.

The organosolv pulping process uses organic solvents such as acetone and ethanol to hydrolyze linkages between lignin with cellulose and hemicelluloses, with minimal changes to the structure of lignin. The organosolv process typically yields lower molecular weight lignins with higher purity and lower hydroxy contents than those obtained by sulfite, kraft, and soda pulping.²⁹ The isolation process strongly influences the applications that a certain lignin variety can be used with; for instance, liginosulfonates are better suited to act as dispersants or stabilizers, while kraft and organosolv lignins can be used to make bio-based polymers.^{30,29}

1.2.3 Lignin Valorization

Over 100 million tonnes of technical lignin are produced every year, amounting to a market size over 900 million USD; these are typically produced as byproducts of chemical pulping and bioethanol production.^{30,31} Lignin's phenolic structure, abundance, and low cost make it an ideal candidate for use in a wide variety of value-added products. Lignin can be processed to make carbon fiber, biofuels, and fine chemicals like vanillin. In recent years, lignin's sustainable nature and low acquisition cost have made it an especially attractive candidate for replacing petrochemicals in bio-based polymeric materials, such as phenolic and epoxy resins.^{32,33}

1.3 Lignin-based PU Flexible Foams

Due to its unique physical properties, sustainability, low cost, and abundant hydroxyl groups, lignin has become an attractive feedstock as a polyol for PU materials.³⁴ Extensive research has been undertaken to develop elastomers,³⁵ adhesives,³⁶ coatings,³⁷ and rigid foams using lignin as a bio-based polyol. Lignins are particularly well suited to rigid foams due to their high hydroxy content and phenolic backbone, which adds strength and rigidity to foams. Manzardo et al.³⁸ performed a life cycle assessment (LCA) which indicated that using lignin in

rigid PU foams can reduce carbon dioxide emissions by up to 30% compared with petroleum-based materials. However, other authors have indicated that the lignin content in PU foams must be greatly increased to significantly reduce GHG emissions of lignin-based foams.³⁹

Several recent studies from our group at Michigan State have developed rigid PU foams with lignin as a polyol replacement. In one study, Henry et al.^{40,41} replaced 80% of a petroleum-derived polyol with fractionated lignin in a rigid foam formulation, resulting in superior mechanical properties compared to a foam made with only petrochemical-derived materials.⁴² Another study by Henry et al.⁴³ showed that 100% replacement of the petroleum- polyol with an unmodified kraft softwood lignin significantly increased the fire resistance of the foam.

Table 1 shows that research on the use of lignin in flexible PU foams is relatively limited; in the past ten years, as of writing, only 16 papers have been published on flexible PU foams using lignin, whereas hundreds of papers have discussed lignins used in rigid PU foams.³¹ While lignin can impart excellent mechanical strength on materials, its high glass transition temperature and crosslinked structure can reduce the flexibility, resilience, and ultimate elongation of flexible PU foams. This has impeded incorporation of lignin into flexible PU foams.

Table 1. Literature on lignin-containing flexible PU foams

First Author	Year	Lignin Type	Lignin Modification Strategy for Foam Synthesis	Lignin Content of Foam (wt%)
Jeong ⁴⁴	2013	Kraft softwood	None	10-20
Cinelli ⁴⁵	2013	Kraft softwood	Microwave Liquefaction with glycerol and PEG	6-13
Bernardini ⁴⁶	2014	Oxypropylated kraft softwood	Oxypropylation followed by microwave liquefaction	6-13
Bernardini ⁴⁷	2015	Soda Herbaceous	Microwave Liquefaction with glycerol and glycerin polyglycidyl ether	8-15
Wysocka ⁴⁸	2016	Lignosulfonate Softwood	Hydrolysis	8-18
Bernardini	2017	Hydrolyzed Herbaceous	Microwave liquefaction	6-12
Gomez-Fernandez ⁴⁹	2017	Kraft softwood	Isocyanate Functionalization	2-10
Gomez-Fernandez ⁵⁰	2018	Soda Herbaceous	None	3-5
Wang ⁵¹	2019	Alkali softwood	Grafting PEG to Lignin	7-16
Zieglowski ⁵²	2019	Kraft softwood	Isocyanate Functionalization	2-3
Maillard ⁵³	2021	Kraft softwood	None	11
Gondaliya ^{54,55}	2021	Multiple	None	14
Ajao ⁵⁶	2021	Soda, bark lignin	None	20
Gurgel ¹⁶	2021	Black Liquor (Kraft)	Transesterification with Castor Oil	1-2
Quan ⁵⁷	2022	Kraft hardwood	None	14
Wang ⁵⁸	2023	Enzymatic Hydrolysis, Herbaceous	Liquefaction with glycerol and PEG using sulfuric acid	-

Gondaliya and Nejad^{54,55} studied the effect of directly incorporating unmodified solid lignin powder into flexible PU foams. In that study, 15 different lignins obtained from various sources (hardwood, softwood, and annual crops), and isolation processes (kraft and organosolv) were used to replace 20% of polyol (20 parts per hundred polyol, pphp) of flexible PU foams. Statistical modeling revealed that there was a strong positive correlation between the total hydroxyl content of lignin and foam density and CFD values, and an inverse correlation between the total hydroxyl content of lignin and ultimate elongation. However, there was no significant correlation between the various OH moieties and foam properties. Lignins with higher hydroxyl content would be expected to increase the crosslinking density in foams, which in turn can result in smaller cell sizes and thicker struts between cell walls, increasing density and strength, but at the cost of ultimate elongation. Furthermore, it was found that lignin-containing foam increased the compression set of the flexible PU foams; TGA analyses showed that lignin increased the thermal stability of flexible PU foams. This study suggested that organosolv lignins are more suitable for flexible PU foams, due to their lower hydroxyl values, better solubility in long-chain polyether co-polyols, and lower glass transition temperature..

Peng et al.⁵⁷ comprehensively studied the effects of lignin isolation processes on lignin-flexible PU foams, by varying the recovery media, pH, temperature and reaction duration of a black liquor refinement process, to produce kraft lignin with various properties. Those lignins were used by our group to prepare PU flexible foams. It was found that the recovered lignin's various molecular weight and dispersities had a statistically significant correlation with foam density and compression force deflection, tensile strength, compression set, and support factor. The best foam properties (e.g., high compression and tensile strength) were achieved with when

the recovered lignin had a relatively low number-average molecular weight (M_n), at 1600 Da, and dispersity (1.8), recovered by using acetic-acid neutralized methanol as a recovery medium.

Wysocka et al.⁵⁹ directly incorporated up to 30 pphp lignosulfonate and hydrolyzed lignosulfonate into flexible and semi-rigid PU foams, and up to 100 pphp lignin into rigid foams. Hydrolysis of lignosulfonate resulted in a higher hydroxyl content due to the cleavage of ether linkages. They reported that the unmodified lignosulfonate foams significantly increased the specific modulus of the foams. Despite the lignosulfonate foams having a higher hydroxyl content, the foams containing hydrolyzed lignosulfonate retained a low specific modulus that was not significantly different compared to the reference foam.

However, there are some major drawbacks with using solid lignin in foam; solid lignin particles tend to act as a filler, rather than a true polyol replacement,⁵⁴ and most PU foam manufacturing plants use liquid streams of polyols, catalysts, and isocyanates, making large scale production of foams with powdered lignin unfavorable to industrial production. Furthermore, lignin's phenolic hydroxy compounds are less reactive towards isocyanates than aliphatic hydroxy groups, while its highly branched structure impedes mobility of polymer chains, reducing flexibility. As a result, lignins used as polyols in flexible foam formulations should be modified so that they are liquid, have mostly aliphatic hydroxyl groups, and are functionalized with linear polymer chains that improve flexibility.

Wang et al.⁶⁰ formulated liquid lignin polyols by grafting polyethylene glycol (PEG) 2000 onto alkali lignin; this was achieved by functionalizing PEG 2000 with epichlorohydrin, followed by subsequent etherification on lignin's phenolic hydroxyl group. This reduced the hydroxyl value of the lignin from 241 to 199 mg KOH/g. High resilience flexible foams were then prepared by reacting the grafted lignin polyol with hexane diisocyanate. However, the

foam's tensile strength and ultimate elongation were not reported, and the foam appeared to have a largely close-celled structure. Interestingly, FTIR and DSC analysis suggested that lignin's structure sterically hinders the formation of ordered hard domains in PUs. In contrast to a foam prepared with ungrafted lignin, foams prepared with PEG2000-grafted lignin showed no aggregation of lignin particles. It was observed that the foam prepared with a PEG2000-grafted lignin polyol had much higher compression moduli, compression force deflection values, and an elastic recovery exceeding 93%. The improved mechanical performance compared to a traditional foam and a foam made with unmodified lignin was attributed to lignin's phenolic structure, which increases the hard segment content, and the improved crosslinking density and interfacial compatibility achieved by grafting with PEG 2000. One counterintuitive result of this study was that foams prepared with PEG2000-grafted lignin appeared to have higher closed cell content, but still maintained a high elastic recovery.

One common strategy for making liquid lignin polyols is liquefaction, which involves partial depolymerization of lignin by cleaving its chemical bonds using thermal energy. Many liquefaction methods are available, including pyrolysis, solvolysis with organic solvents, hydrothermal liquefaction with water, and cleaving with hydroxy radicals.⁶¹⁻⁶⁴ Lazzeri's group was the first to report a flexible PU foam utilizing lignin as a polyol in 2013. Indulin AT Kraft-Softwood lignin underwent liquefaction by mixing lignin with glycerol and PEG 400 (polyethylene glycol, $M_n = 400$ Da) under a microwave treatment; the resulting liquid lignin polyols had OH values ranging from 360-370 mg KOH/g, requiring the use of additional long-chain diols to act as chain extenders in the final foam. DMA analysis showed that the $\tan \delta$ of the soft phase diminished in intensity with increased lignin content, indicating that the polyol chains of the soft segment underwent phase mixing with the lignin-polyol in the hard-segment; this was

attributed to lignin's phenolic structure. Additionally, higher lignin contents were associated with significantly higher storage moduli.⁶⁵

Oxyalkylation of lignin with alkylene oxides was first introduced by Glasser⁶⁶ and remains a common technique for production of lignin polyols, and it is one of the most common methods for synthesizing rigid lignin-based PU foams.⁶⁷⁻⁷⁰ This technique is particularly useful for polyol production as it replaces the sterically hindered and less reactive phenolic OH groups on lignin with a low glass transition, polyether backbone with terminal aliphatic OH groups that are more reactive towards isocyanates. Another study by Lazzeri's group continued the work on liquefacted lignin in flexible PU foams, but first oxypropylated lignin prior to liquefaction with PEG 400 and subsequent foam formulation. They reported mostly minimal changes overall to foam properties, but indicated that oxypropylated lignin had higher miscibility with bio-based co-polyols, especially castor oil, and that oxypropylated lignin contributed to a higher soft-domain content, based on DMA data. Additionally, foams prepared with oxypropylated lignin and castor oil as a co-polyol showed slightly lower compression force deflection (CFD) values, ranging from compared to those made with unmodified lignin; this was attributed to lignin degradation during the oxypropylation step.

In summary, there have been several attempts to develop lignin-based PU flexible foams over the past 15 years. However, in all of these cases, the amount of lignin within the final foam is limited to 20%. There has been some success in using solid lignin powder to replace up to 20 wt% of a PU foam, but in those instances lignin acts partially as a filler, meaning that they do not fully react with isocyanates. Additionally, liquid polyols are preferred by industry for scale up. However, most of the methods for developing liquid lignin polyols, including liquefaction and oxypropylation, are energy and chemically intensive. For instance, alkylene oxides, used in

lignin oxypropylation, are volatile, flammable, and carcinogenic petroleum based chemicals, in addition to being largely petroleum derived.

One promising approach for producing lignin polyols is oxyalkylation using cyclic alkylene carbonates in place of alkylene oxides; this strategy has not yet been attempted in flexible foams. This approach was first introduced by Kuhnel et al.,^{71,72} while Dr. Nejad's group recently patented the production of liquid lignin polyol solutions with this technology.^{73,71,72} Cyclic alkylene carbonates like propylene carbonate and ethylene carbonate are classified as green solvents because they are non-toxic, have high boiling points, low vapor pressures (they are considered to be "VOC-exempt" by the US EPA), are bio-degradable, and have excellent solubility with a wide range of materials.⁷⁴ Cyclic carbonates thus represent an attractive alternative to alkylene oxides for synthesizing oxyalkylated lignin polyols.⁷⁵ A potential benefit of the use of cyclic carbonates in PU formulations is the incorporation of carbonate groups into the soft segment, which has been reported to improve mechanical properties and resistance to hydrolysis.^{76,77} Additionally, because cyclic carbonates can be synthesized from carbon dioxide, they can further reduce the greenhouse gas emissions of lignin-based PU foams.⁷⁸ Optimization studies of this process determined that 1,8-diazabicyclo(5.4.0)undec-7-ene (DBU) yielded a higher conversion and degree of polymerization compared to other basic catalysts including potassium carbonate, dicyanodiamide, and 1,4-diazabicyclo(2.2.2)octane.^{72,79} A few studies have begun to use cyclic-carbonate oxyalkylated lignin in rigid foams and adhesives.⁸⁰⁻⁸² The primary objective of this work is to develop liquid lignin polyol via oxyalkylation of lignin with propylene carbonate, and to then incorporate them into flexible PU foam formulations.

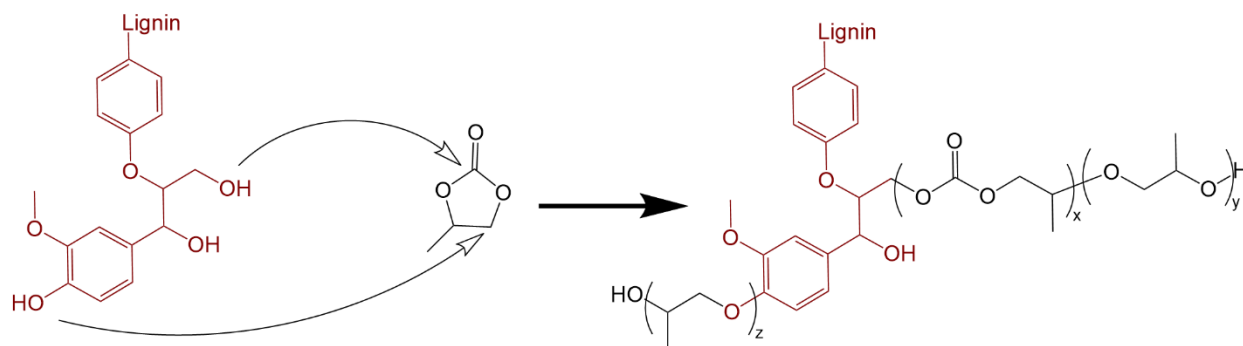


Figure 6. Oxypropylation of lignin with propylene carbonate

1.4 Application of Computational Chemistry to Lignin-Polyurethane (PU) Systems

While lignin contains many OH groups that have the potential to bond with isocyanate groups, these OH groups can have very different electronic environments, which affect their ability to bond with isocyanate groups. In addition, due to the 3D complex structure of lignin, not all OH groups are available for reaction. Previous work⁸² by Dr. Nejad's group at MSU further investigated various lignin's reactivity with isocyanates, using lignin model compounds representing the various OH moieties present in lignin.⁸³ This study used NMR and FTIR analysis to show that the reactivity of lignin OH moieties with isocyanate followed the trend: aliphatic > H > G > S > carboxylic acid. Interestingly, it was demonstrated that there was minimal significant differences in the reactivities of S and G groups. A goal of this project will be to use quantum mechanical simulations to further investigate how different types of hydroxy groups affect the reaction kinetics of the lignin-isocyanate reaction. Density Functional Theory (DFT) is a widely used computational chemistry technique that can model the electronic structure of complex systems like molecules and crystals. The basic working principle of DFT is that the energy of a quantum system can be defined as functional (a function of another function) of electron density. Thus, rather than solving for the wave function of each electron in a

molecule, DFT can approximate the properties of molecules using electron densities, which requires much less computational time.

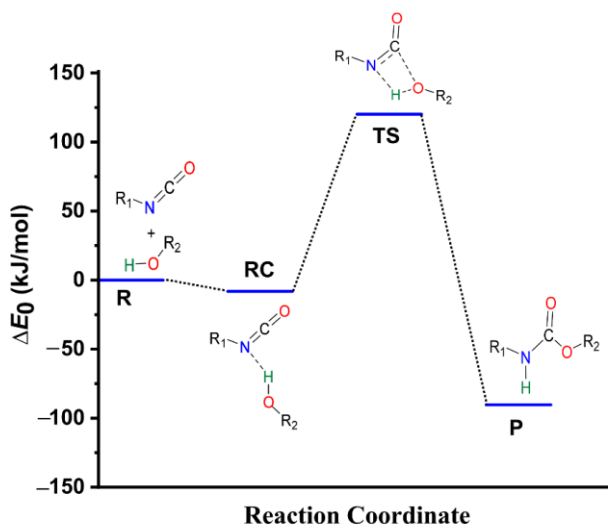


Figure 7. Reaction coordinate diagram of the urethane formation reaction. Reproduced from Waleed et al.⁸⁴

Since the 2010s, a great deal of research has been published using DFT to study both PU and lignin. For instance, several studies have successfully modeled the urethane formation reaction in simpler systems using methanol and phenyl isocyanate.^{85–87} In general, there are 3 stages to the uncatalyzed urethane reaction; first, a hydrogen bond forms between the nitrogen of the isocyanate and the hydrogen of a hydroxyl group. Then, as the reaction proceeds, an unstable transition state (TS) forms. After this stage, the hydrogen transfers from the hydroxy group to the nitrogen, and the reaction proceeds to form a urethane structure. One computational study determined that the uncatalyzed reaction barrier for the methanol-phenyl isocyanate reaction is 120 kJ/mol.⁸⁴

Lignin has a highly irregular, crosslinked, and amorphous structure with a high molecular weight. As a result, it can be very computationally expensive to model lignin for quantum

mechanical and molecular dynamics simulations. Typically, small model compounds containing a combination of lignin monomers with linkages typically found in lignin are used to approximate reactions with lignin. For instance, one study used a 1,3-diarylpropan-1,2-diol derivative as a lignin model compound with a B3LYP functional to evaluate the reactivity of lignin toward different kinds of isocyanates.⁸⁵

Most computational studies on lignin and the urethane reaction have used hybrid functionals that combine DFT with the more advanced Hartree-Fock method. However, hybrid functionals have a very high computational cost, which is exacerbated by lignin's large and complicated structure. One study found that using the Perdew-Burke-Erznherhoff (PBE) functional, a generalized gradient approximation (GGA) method, was still able to produce reasonably accurate results in lignin systems with a much lower computational cost.⁸⁵ Additionally, because these lignin model compounds are non-periodic, molecular systems, most of the relevant studies use Gaussian basis sets.⁸⁷

1.5 Objectives

The main objective of the present work is advancing the use of lignin in flexible PU foams and understanding how using liquid lignin polyol with only aliphatic hydroxy groups can improve foam performance compared to solid lignin. To that end, this study can be divided into three segments.

- Perform a small-scale computational study to determine if the lignin-isocyanate reactions can be accurately modeled with Density Functional Theory (DFT) computations.
- Assess the effects of different lignin varieties on the properties of liquid lignin polyols synthesized with propylene carbonate as a green solvent and oxyalkylation reagent.
- Partially replace polyols in a flexible foam formulation with liquid lignin polyols.

- A major design goal of this project was to develop PU foams with at least 20% replacement of petroleum-based polyol with liquid lignin polyols, which met standard mechanical properties for automotive seating applications.
- A secondary goal was to assess the structure-property relationships of the synthesized PU foams.

CHAPTER 2 Materials and Methods

2.1 Materials

Lignin samples were provided by Fortum, West Fraser, Sweetwater Energy, Advanced Biochemical Thailand, Ingevity, and Greenvalue Enterprises. 1,8-Diazabicyclo(5.4.0)undec-7-ene (DBU) was purchased from Tokyo Chemical Industry (TCI). Propylene carbonate, Rubinate M polymeric methylene diphenyl diisocyanate (pMDI), XC3000 amine gelation catalyst, XC1000 amine blowing catalyst, XC7000 balance catalyst, and XS068 siloxane surfactant were provided by Huntsman. A polyether polyol, with functionality 3 and $M_n = 4000$ Da, was provided by Woodbridge Foam.

For ^{31}P -NMR analysis and GPC analysis, cyclohexanol (99% purity), pyridine (HPLC grade), and 2-chloro-4,4,5,5-tetramethyl-1,3,2-dioxaphospholane (TMDP) were purchased from Sigma-Aldrich. Chromium(III) acetylacetonate, deuterated chloroform, HPLC-grade tetrahydrofuran, and acetic anhydride were obtained from Fisher.

2.2 Computational Methods

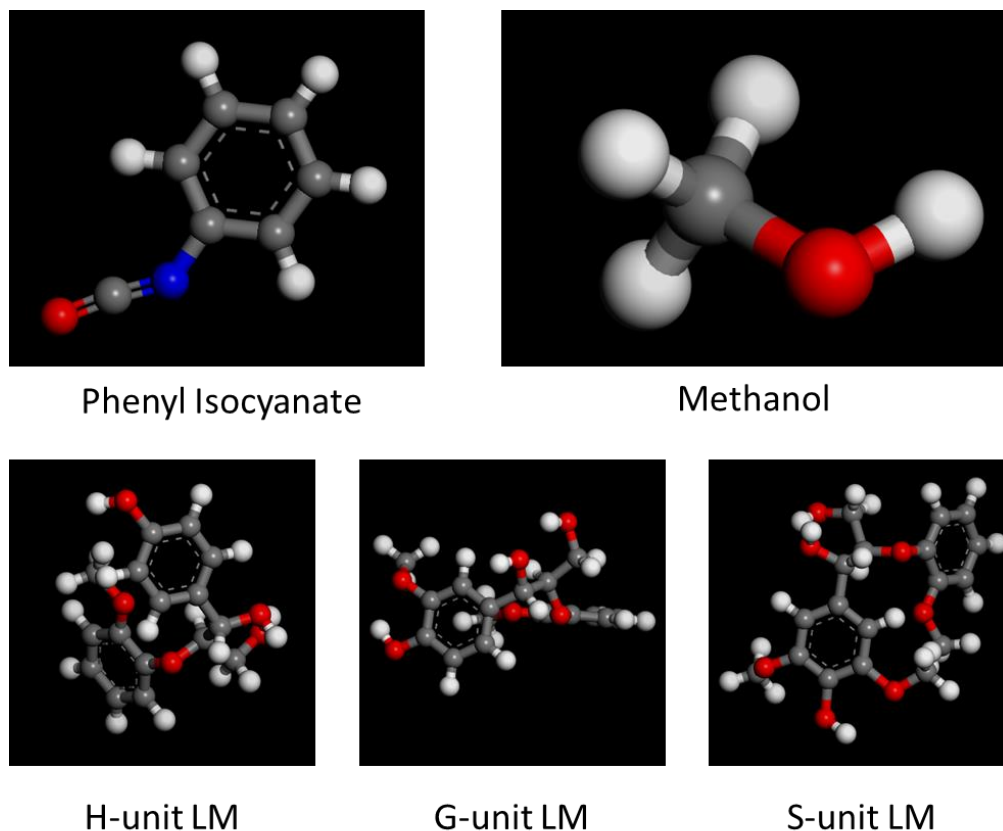


Figure 8. Materials Studio 3D models of phenyl isocyanate, methanol, and three lignin model compounds containing H, G, and S units

Density functional theory (DFT) calculations, using Biovia Materials Studio software, were used to investigate how the different types of lignin hydroxy (OH) groups react affect the reaction profile of the urethane formation reaction. As shown in the Figure 8, derivatives of 1,3-diarylpropan-1,2-diol were used as lignin model (LM) compounds; this compound is derived from two guaiacyl (G) units and contains both aliphatic and phenolic OH groups. These compounds are dimers of lignin monomers; the three lignin monomers were not used because they contain unsaturated double bonds, while natural lignin mostly contains saturated bonds. Similar lignin model compounds were used by Zieglowski et al.⁵² when using DFT to investigate

lignin's reaction with various isocyanates. By modifying the amount of methoxy groups on the ortho position of the phenolic ring, 3 different model compounds, with G, H, and S units were created. The G-unit model compound was also used to investigate reactions of phenyl isocyanate with lignin's primary and secondary aliphatic hydroxy groups. Methanol was also used as a model hydroxy compound, for comparing our results with previously published papers. Phenyl isocyanate was used as the model isocyanate compound because it has an aromatic structure that is similar to the diisocyanates (TDI and pMDI) commonly used in PU foam applications). Simulations were carried out using the DMol³ program within Biovia Materials Studio⁸⁸, using a Perdew-Burke-Ernzerhoff (PBE) functional, which is based on the general gradient approximation (GGA). A double-numerical + polarization (DNP) basis set was used because it adds "d" polarization functions to all non-hydrogen atoms and a "p" orbital polarization function to H-atoms. This is important for accurately modeling hydrogen bonding,⁸⁸ which plays a critical roles in PU reactions.⁸⁴

Six total simulations were performed, corresponding to reactions of phenyl isocyanate with methanol and the lignin model compound's primary aliphatic, secondary aliphatic, p-hydroxyphenyl (H), guaiacyl (G) and syringyl (S) hydroxy structures. 3D atomistic documents were created with a urethane linkage between phenyl isocyanate and the relevant hydroxy groups for each compound. A geometry optimization algorithm was applied to phenyl isocyanate, methanol, the 3 lignin model compounds, and the 6 different urethane-containing structures to determine the ground state energy for each structure; the collected data was used to calculate the reaction energy released during the formation of each urethane linkage. To predict the activation energy barriers, one 3D atomistic document was created with phenyl isocyanate positioned near the relevant hydroxy group, and paired with the corresponding urethane structure document

using the reaction preview tool in Materials Studio, to create a reaction trajectory document. Lastly, a transition state search was run for each reaction trajectory in Dmol3, using linear and quadratic synchronous transit methods (LST/QST).⁸⁹ This algorithm works to find the saddle point of the potential energy surface of the predicted reaction trajectory, which corresponds to the transition state. To achieve comparable results with literature^{84,90}, an implicit solvent model, using acetonitrile as the simulated solvent, was used during the transition state search.

2.3 Lignin Characterization

All lignin samples used in this study were characterized to understand their chemical structure and physical properties.

2.3.1 Ash Content

The ash contents of lignin samples were measured according to a standard method described in TAPPI T 212 om-9.⁹¹ Briefly, each oven-dry lignin sample (1–2 g) was added to a pre-weighed crucible and heated in a muffle furnace. The temperature was gradually increased from room temperature to 525 °C at a ramp rate of 5 °C min⁻¹ and then kept at 525 °C for 4 h. After cooling in a desiccator, the ash content was determined as the ratio of residual mass in the crucible compared to the initial mass of the dry lignin.

$$\text{Ash Content (wt\%)} = \frac{m_{\text{crucible},f} - m_{\text{crucible},i}}{m_{\text{crucible},i}} \times 100\% \quad [1]$$

2.3.2 Elemental Analysis

Lignin samples were dried overnight at 100-105 °C, ground with a Wiley Mill, and sieved through a number 10 sieve (2 mm). All lignin samples were prepared according to Association of Official Analytical Chemists (AOAC) Official Methods 922.02 and 980.03, and sent to an external laboratory to perform Inductive-Coupled Plasma Atomic Emission Spectroscopy (ICP-AES) with a Thermo Scientific iCAP 6000 series 6500 Duo.

2.3.3 Phosphorous 31 Nuclear Magnetic Resonance Spectroscopy (^{31}P -NMR)

The hydroxy contents and chemical structure of lignin and synthesized lignin polyols were analyzed according to an established procedure.⁹²⁻⁹⁵ A solution of HPLC grade pyridine and chloroform-d (1.6:1, v/v) was prepared as a solvent. Approximately 22 mg (precisely measured) of cyclohexanol was dissolved in 1 mL of the solvent to prepare an internal standard solution. 5-7 mg of chromium (III) acetylacetonate was dissolved in 1 mL of the solvent, and approximately 35 mg of the lignin sample was dissolved in 500 μL of the prepared solvent. All prepared solutions were mixed for 30 s in a vortex at 3000 rpm. 100 μL of the chromium (III) acetylacetonate solution and 100 μL of the internal standard solution were added to the lignin solution. Next, 100 μL TMDP was added to the lignin solution, and mixed for 30 s in a vortex at 3000 rpm. The samples were then transferred to a 5mm Wilmad NMR tube. The NMR solution was analyzed in an Agilent DDR2 500 MHz NMR spectrometer equipped with 7600AS, running VnmrJ 3.2 A. Data was collected using a 90° pulse angle with a relaxation delay of 5 s, and 128 scans. Hydroxy contents were quantified using MNova software (Mestrelab), by computing ratios of integrated areas around the cyclohexanol peak (145.3-144.9 ppm) to the various lignin hydroxy moieties: aliphatic (149.1-145.4 ppm), condensed phenolic (144.6-143.3 and 142.0-141.2 ppm), syringyl phenolic (143.3-142.0 ppm) guaiacyl phenolic (140.5-138.6 ppm), *p*-hydroxyphenyl phenolic (138.5-137.3 ppm) and carboxylic acids (125.9-134.0 ppm). Equation 2 describes the calculation of the internal standard integrated peak area; 0.1 is the dilution factor, 0.99 is the purity of the internal standard, and 100.158 refers to the molar mass of cyclohexanol.

$$IS\ area\ (mmol/g) = 0.1 \times 0.99 \times \frac{m_{IS}(mg)}{m_{lignin}(mg)} \times \frac{1000(mmol/mol)}{100.158(mol/g)} \quad [2]$$

2.3.4 Gel Permeation Chromatography (GPC)

The molecular weight distributions of the lignin samples were measured by performing gel permeation chromatography (GPC), using tetrahydrofuran (THF) as the mobile phase. To completely solubilize lignin in THF, the samples were acetylated by mixing 1 g lignin in 40 mL of a pyridine-acetic anhydride solution (50-50 v/v%) for 24 hours at room temperature. The samples were precipitated with 0.1 M hydrochloric acid, washed with deionized water 3 times, and dried in a vacuum oven. The samples were then dissolved in HPLC grade THF at a concentration of 5 mg/mL, and the solution was filtered using a 0.45 μm syringe filter.

The filtrate was injected into the GPC system (Waters, Milford, MA, USA), including a separations module (Waters e2695). The mobile phase was THF (HPLC grade), with a 1 mL min⁻¹ flow rate. Three 300 mm \times 7.8 mm Ultrastyrigel columns from Waters (100–10 K, 500–30 K, and 5 K–600 K Å) with THF as the mobile phase were used. Polystyrene standards with molecular weights of 162, 370, 474, 580, 945, 1440, 1920, 3090, 4730, 6320, 9520, 16700, and 42400 Da were used for calibration. The molecular weights of samples were calculated using Empower GPC Software.

2.4 Comparative Analysis of Liquid Lignin Polyols from Different Lignin Varieties

2.4.1 Synthesis of Lignin Polyols

Eleven different lignin polyols, using lignins from various biomass sources and isolation processes were synthesized to gain a better understanding of the relationship between lignin and polyol properties. Polyols were synthesized by reacting propylene carbonate with lignin, using a 1:10 molar ratio of lignin hydroxy groups per propylene carbonate (PC) molecule.

Diazabicyclo(5.4.0)undec-7-ene (DBU) was used as a catalyst, with a molar ratio of 0.05 moles DBU per 1 mole of lignin hydroxy groups.⁷³ Table 2 displays the synthesis parameters for each

lignin polyol. 50 grams of lignin and the calculated amounts of DBU and propylene carbonate were charged into a 600 mL Parr Reactor, which was purged with dry nitrogen gas for 30s. The reactions proceeded for 6 hours at 150 °C in a nitrogen atmosphere, mixing with a propeller at 300 rpm. After the reaction finished, the reactor vessel was quenched in cold water and lignin polyols were stored in polypropylene flasks.

Table 2. Synthesis Parameters of Liquid Lignin Polyols

Lignin ID	Sources	Processing	Lignin OH Content (mmol/g)
1-K-SW	Softwood	Kraft	5.77
2-O-SW	Softwood	Organosolv	4.12
3-O-HW	Hardwood	Organosolv	4.88
4-O-CS	Corn Stover	Organosolv	3.89
5-S-WS	Wheat Straw	Soda	5.46
6-K-HW	Hardwood	Kraft	5.92
7-S-HW	Hardwood	Soda	6.56
8-O-WS	Wheat Straw	Organosolv	3.53
9-K-HW	Hardwood (Eucalyptus)	Kraft	6.66
10-K-SW	Softwood	Kraft	4.66
11-O-WS	Wheat Straw	Organosolv	3.73

2.4.2 Characterization of Lignin Polyols

2.4.2.1 Hydroxy Value Determination

The hydroxy contents of lignin polyols were measured using ^{31}P -NMR spectroscopy, using a method identical to that used for lignin characterization. The hydroxyl value (OHV), a measure of the free hydroxy groups in a substance, which is normally determined via titration with potassium hydroxide of an acetylated sample, was computed using ^{31}P -NMR data by using by equation 3; the active hydrogen equivalent weight (AHEW), was computed as the inverse of the total hydroxy content (equation 4).

$$\text{Hydroxy Value (OHV)} = \text{Total Hydroxyl Content (mmol/g)} \times 56.1 \quad [3]$$

$$\text{AHEW} = \frac{1000}{\text{Total Hydroxyl Content (mmol/g)}} \quad [4]$$

2.4.2.2 Viscosity

The viscosity of the lignin polyols were measured using a Discovery HR-1 hybrid rheometer from TA Instruments, using a 40 mm stainless steel Peltier plate geometry, with a 1 mm gap. Samples were placed between the plates and trimmed prior to measurement. The viscosity was measured at a constant shear rate of 50 s^{-1} , taken as the average viscosity over a 5 second interval.

2.4.2.3 Unreacted Propylene Carbonate (PC) Content

The unreacted PC content of the lignin polyols were measured gravimetrically to determine the proportions of modified lignin and residual propylene carbonate after the reaction. The mass of a dry 50 mL beaker and a Pyrex ASTM 10-15 M Gooch Crucible were measured. 1 g of each polyol was dropped into a beaker with 20 mL water and vigorously stirred for 1 minute; the precipitated lignin and solution were then vacuum filtered using the filter crucibles. The samples (both in the beaker and Gooch crucible) were then left to dry overnight at $105 \text{ }^\circ\text{C}$, and placed in a desiccator to cool. The unreacted PC content of the polyols was determined by equation 5.

$$\text{Unreacted PC (wt\%)} = \left(1 - \frac{\Delta m_{\text{beaker}} + \Delta m_{\text{crucible}}}{m_{\text{lignin polyol}}}\right) \times 100\% \quad [5]$$

2.5 Synthesis and Characterization of Flexible PU Foams with Liquid Lignin Polyols

2.5.1 Liquid Lignin Polyol and Foam Synthesis

Three lignins from different biomass sources and isolation processes were used to prepare lignin polyols with lower ratio of lignin to PC for partially replacing the petroleum-based polyol in flexible PU foams designed for automotive seating applications.

Table 3. Lignins used to synthesize flexible PU foams

Sample ID	Isolation Method	Lignin Source	Supplier	Lignin (g)	Propylene Carbonate (g)	DBU (g)
O-WS	Organosolv	Wheat Straw	Fortum	100	199	3
K-SW	Kraft	Softwood	West Fraser	100	238	3.5
H-HW	Acid Hydrolysis	Hardwood	Sweetwater Energy	100	277	4.1

First, lignin samples were all oven-dried at 80 °C for 24 hours. Lignin was reacted with propylene carbonate in the presence of 1,8-Diazabicyclo(5.4.0)undec-7-ene (DBU) catalyst. 5 moles of propylene carbonate were reacted with every one mole of lignin OH groups, with 0.05 moles of DBU per lignin OH group. To make each polyol, 100 g lignin, and the calculated amounts of propylene carbonate and DBU were charged into a Model 4524 Parr Reactor (2L capacity). The reactor was then sealed and purged with nitrogen gas for 30 s to remove atmospheric moisture. The temperature was then increased to 150 °C and the reaction proceeded for 90 minutes, mixing at a speed of 300 rpm; the pressure was periodically released during the course of the reaction to avoid excess carbon dioxide build-up. Once the reaction had completed, the reactor vessel was quickly quenched with cold water, and the samples were removed. The

lignin polyol properties (hydroxy value, viscosity, and unreacted PC) were characterized by the methods described earlier in section 2.4.2.

Foams were prepared according to the formulation in Tables 4 and 5. In PU foam production, isocyanates are typically referred to as the “A-side”, while polyols, catalysts, and surfactants are typically mixed separately and called the “B-side”. The B-side is typically quantified by parts per hundred polyol (pphp), which refers to the mass in grams of each component per 100 grams of polyol.² For each type of lignin, 10, 20, and 30 pphp of petrochemical polyols were replaced with the lignin polyols to synthesize flexible PU foams. Due to the high hydroxyl value and crosslinked polyphenolic structure of the lignin-polyol, it is not possible to fully replace polyether polyol in flexible foam formulations.

Table 4. Polyol and isocyanate compositions of synthesized flexible PU foams

Sample ID	Lignin Type	Lignin-Polyol (pphp)	Polyether Co-polyol (pphp)	pMDI (pphp)
Control	-	0	90	53
O-WS 10	Organosolv Wheat Straw	10	80	54.4
O-WS 20	Organosolv Wheat Straw	20	70	55.9
O-WS 30	Organosolv Wheat Straw	30	60	57.4
K-SW 10	Kraft Softwood	10	80	55.1
K-SW 20	Kraft Softwood	20	70	57.3
K-SW 30	Kraft Softwood	30	60	59.5
H-HW 10	Acid Hydrolysis Hardwood	10	80	55.5
H-HW 20	Acid Hydrolysis Hardwood	20	70	58.1
H-HW 30	Acid Hydrolysis Hardwood	30	60	60.7
Optimized	Kraft Softwood	20	70	50.2

Table 5. Minor components, including co-polyols, blowing agents, and catalysts used in flexible PU foam formulations

Component	Composition (pphp)
SAN Grafted Co-Polyol	10
Water (Blowing Agent)	4
Gelation Catalyst	0.3
Blowing Catalyst	0.08
Balance Catalyst	0.5
Silicone Surfactant	0.5

The isocyanate (NCO) index, which is the stoichiometric ratio of isocyanate groups per 100 hydroxyl groups in a PU formulation, was set to 80 for all foams (except the optimized foam) to account for the high functionality and hydroxyl content of the lignin polyols.^{46,54} Thus, the mass of isocyanate used was computed by Equation 1. The isocyanate used was, a polymeric methylene diphenyl diisocyanate (pMDI) with an equivalent weight of 133.4 g/eq.

$$m_{A-side} = m_{B-side} \times 0.8 \times NCO \text{ Eq. } Wt \times \sum \frac{pphp_i}{OH \text{ Eq. } Wt.} \quad [6]$$

Additionally, after these foams were synthesized and tested, another foam was created with a slightly modified formulation that was designed to meet all the required mechanical property standards for automotive seating. The collected data, as discussed in the results section, indicated that the foam with 20 pphp K-SW lignin polyol had mechanical properties that best matched those of the control formulation, but had a lower ultimate elongation than required for automotive seating locations. To alleviate this issue, an “optimized” foam with a reduced isocyanate index of 70 was synthesized and tested.

To prepare foam samples for mechanical testing, 120 g polyol (including both polyether polyol and lignin polyol) and the calculated amount of catalysts and surfactants were mixed for 2 min at 3000 rpm in a 12 oz paper cup. Then, the calculated amount of isocyanate was added

using a needle-less plastic syringe, and mixed with the B-side at 3000 rpm for 3-5 seconds. The polyol-isocyanate mixture was then quickly poured into a 30 x 30 x 5 cm silicone mold that had been heated to 65 °C. After 2 minutes of curing, the foams were removed from the mold and left to cure for 48 hours. After post-curing, a band saw was used to remove 1 cm of skin from the foam and to cut the foam into mechanical testing specimens.

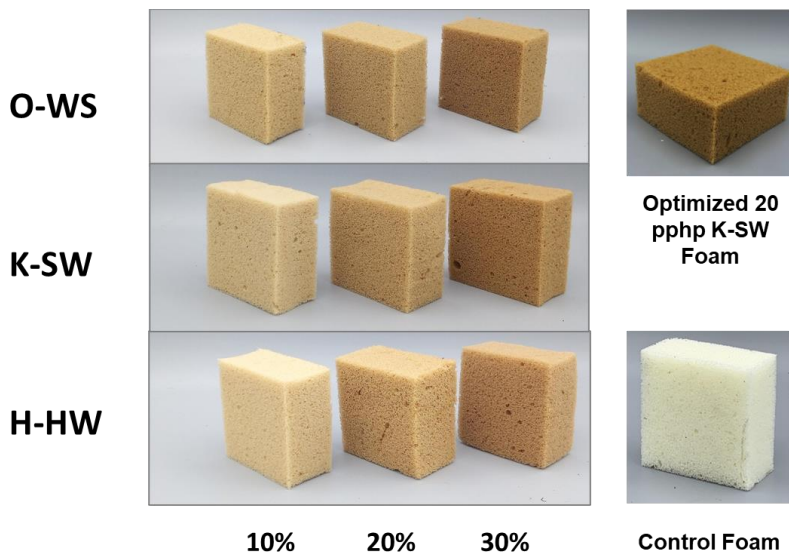


Figure 9. Foam samples partially synthesized with various lignin polyols

2.5.2 Characterization of Flexible PU Foams

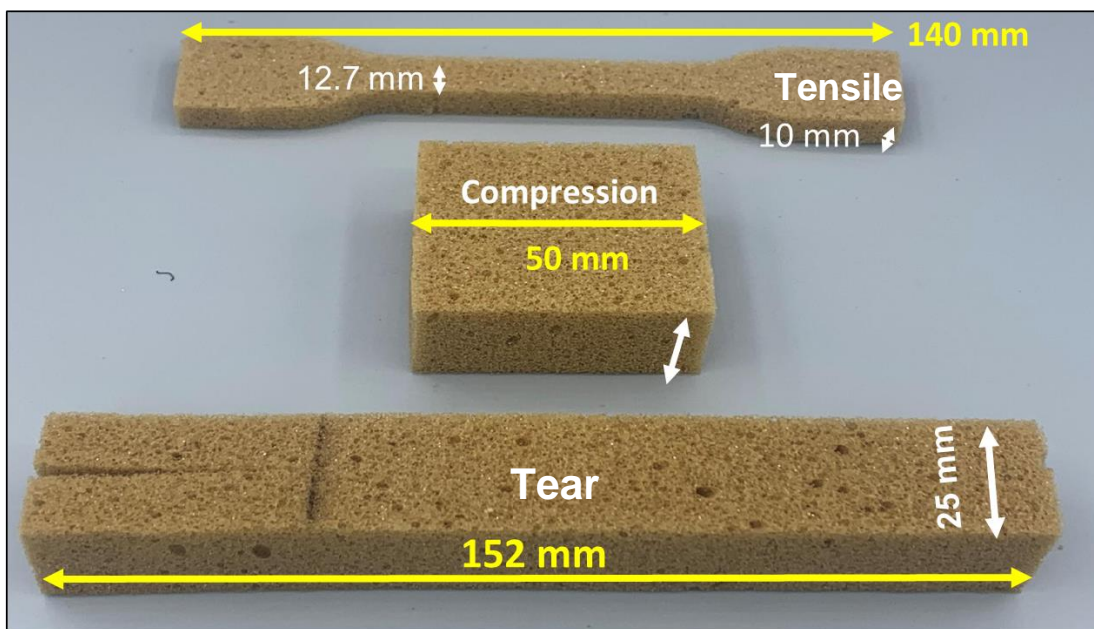


Figure 10. ASTM 3574 mechanical property testing specimens

2.5.2.1 Reaction Profile

The relative reactivity of each foam was compared using cup tests as specified in ASTM standard D7487-18.⁹⁶ Foams were prepared according to the prescribed formulation, using 15 g of polyol per cup, and 3 replicates per sample. A timer was started when the isocyanate and polyol began mixing. The cream time (when gas bubbles begin appearing), gel time (when long strings of tacky material can be pulled from the foam surface), end of rise time, and tack free time of the foams were recorded.

2.5.2.2 Apparent Density

Using a band saw equipped with scallop blades, foam samples were cut into 50 x 50 x 25 mm blocks. Four replicates were used for this test. Their dimensions were precisely measured to the nearest 0.1 mm with calipers. The samples were weighed on a high precision Mettler-Toledo

balance to nearest 0.001 g, and apparent density was calculated by dividing the samples' mass by its volume.

2.5.2.3 Compression Force Deflection

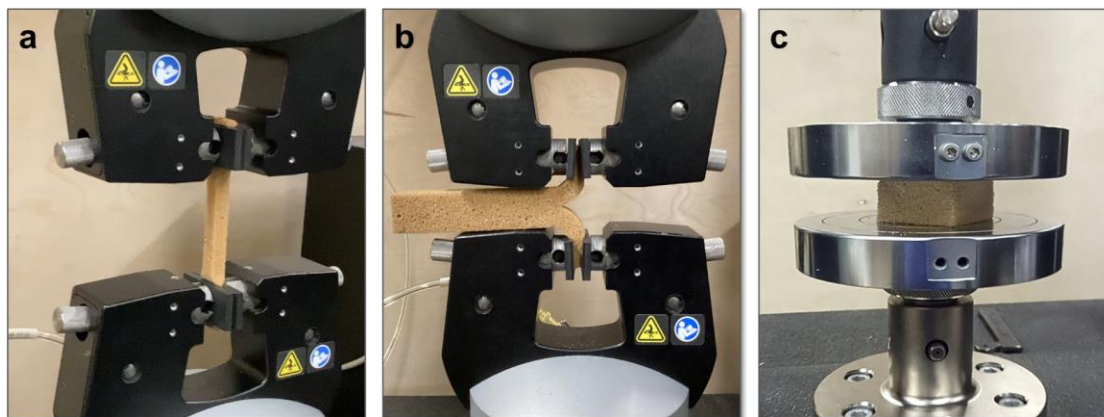


Figure 11. Mechanical testing of flexible PU Foams: a) Tensile Test b) Tear Resistance Test c) Compression Force Deflection (CFD) Test

The same 50 x 50 x 25 mm foam samples used for measuring the apparent densities were used to measure the load bearing properties of the foam. The samples were placed on an Instron universal testing machine equipped with compression platens. The platen separation was set to the foam height (~25 cm). The samples were then compressed to 75% of their initial height as part of “pre-flex” to break any residual closed cells. Then allowed to recover for at least 6 minutes, before pressing them again.

After recovery, the samples were then compressed to 25% strain, and the stress was measured after 1 minute of relaxation. This test was repeated at 50% and 65% strain. The compression force deflection (CFD) was reported as the stress after 1 minute of relaxation at 50% strain. The CFD is directly proportional to foam density, so a density-normalized CFD was also reported. The support (sag) factor was reported as the ratio of the stress at 65% strain to the stress at 25% strain (equation 7)

$$\text{Support Factor} = \frac{\text{CFD at 65\% Strain}}{\text{CFD at 25\% Strain}} \quad [7]$$

2.5.2.4 Tensile Test

The tensile strength and elongation of samples were measured according to ASTM D3574-17, part E. Foam samples were cut to approximately 10 mm in thickness in the rise direction. Then, a hydraulic press was used with a die to cut dog-bone shaped sample specified in ASTM D412A. The width and thickness of the samples were precisely measured with calipers. The samples were then placed into an Instron 5585H universal testing machine, with a 10 kN load cell, and secured with hydraulically controlled rubber grips. The grip separation was 80 mm; this dimension was considered to be the “initial length” for strain calculations. The samples were pulled at a rate of 500 mm/min, and the tensile strength, elastic modulus, and ultimate elongation at break were recorded.

2.5.2.5 Tear Resistance Test

The tear resistance was measured according to ASTM D3574-17 Test F. Foams prisms were cut with dimensions 25.4 x 25.4 x 152.4 mm (1” x 1” x 6”), using at least 4 replicates. A 40 mm slit was cut into the long dimension of the foam, parallel to the foam rise direction; the foam thickness was recorded parallel to this slit. The foam was then placed into an Instron universal testing machine, with each grip holding about 1 cm of each tab made by the slit, as shown in Figure 11b. The sample was then pulled apart at 500 mm/minute, until the tear propagated 120 mm or the tear cut through the foam. The tear strength was computed using equation 8.

$$\text{Tear Strength (N/m)} = \frac{\text{Maximum Force}}{\text{Thickness}} \quad [8]$$

2.5.2.6 *Fourier-Transform Infrared (FTIR) Spectroscopy*

The infrared spectra of control foams and a 30 pphp foam for each lignin type was measured with a PerkinElmer Spectrum Two FT-IR Spectrometer, in Attenuated Total Reflectance (ATR) mode. 10 mm thick foam samples were compressed at the same force-level during measurement to ensure that the ATR crystal maintained adequate contact with the foam. The spectrum was processed with a baseline correction and noise-reduction algorithm after data collection.

2.5.2.7 *Thermogravimetric Analysis (TGA)*

The thermal degradation of the control foam and optimized foam samples were investigated using a TGA55 (TA Instruments) thermogravimetric analyzer. 7-10 mg of each foam sample was placed in a platinum pan and heated to 800 °C at a rate of 10 °C/min. The weight loss % thermogram and its derivative were recorded.

2.5.2.8 *Scanning Electron Microscopy*

The morphology of the control foam, optimized foam, and the 30 pphp foam for each lignin type were investigated using scanning electron microscopy (SEM). Samples were cut with a razor blade perpendicular to the foam rise direction. Then, the samples were mounted using carbon tape and sputter coated with gold nanoparticles in an argon atmosphere to allow the samples to be conductive. Images were collected on a JEOL 6610LV SEM, with an accelerating voltage of 10 kV and a spot size set to 30. Images were collected at 50x, 100x, and 1000x magnification. Low magnification images were taken with SEM instead of optical microscopy because the 3D structure of foam requires a much larger depth of field than can be provided with optical microscopy.⁹⁷

2.5.2.9 *Dynamic Mechanical Analysis (DMA)*

Foam samples were subjected to dynamic mechanical analysis (DMA) in compression mode. The main purpose of this test was to examine how the lignin-polyols affect the soft-segment glass transition. Cylindrical samples with diameters of 20 mm and thicknesses of 10 mm were cut from bulk foam samples. The test parameters were a 50 μm amplitude test (confirmed to be in the linear elastic regime by a linear-oscillation test), a 0.044 N preload force, and a 1 Hz frequency. Samples were cooled to 100 °C and the storage modulus, loss modulus and $\tan \delta$ were collected over a temperature range of -90 to 100 °C.

2.5.3 *Partial Least Squares-Regression Modeling*

Partial least squares regression (PLS-R) modeling was used to model relationships between lignin, polyol properties, and foam performance. A four component model was developed using SIMCA 18 chemometric modeling software, with lignin and polyol properties as the predictor variables, and the mechanical properties of the foam as the response variables. Several of the predictor variables were crossed (meaning the factors were multiplied together) with the lignin-polyol content in each foam. The idea was that because the foams were collected with 10, 20, and 30 pphp, crossing the LP content of the foam with another variable (like the lignin Mn) would indicate if that variable affected the foam performance.

CHAPTER 3 Results and Discussion

The results of the three main experiments are presented here. First, the computed activation and reaction energies of the lignin-isocyanate reaction were tabulated and compared to experimental results. Then, the properties of lignin-polyols made with propylene carbonate and different lignin varieties were investigated. Lastly, 3 lignin polyols, made using lignins from different biomass sources and isolation processes, were used to partially replace the polyol portion of flexible polyurethane (PU) foams, and the structure and mechanical properties of these foams were extensively investigated.

3.1 Computational Modeling of the Lignin-Isocyanate Reaction

Density Functional Theory (DFT) modeling was used to predict the reaction-energy profile of the lignin-isocyanate reaction. Both the reaction energy and activation energy were calculated when phenyl isocyanate reacted with various types of hydroxyl (OH) groups present in lignin. Figure 29 in the Appendix demonstrates how the Linear Synchronous Search (LST) algorithm extrapolates a reaction trajectory from the product and reactant files, and probes the energies at different points to approximate an activation energy.

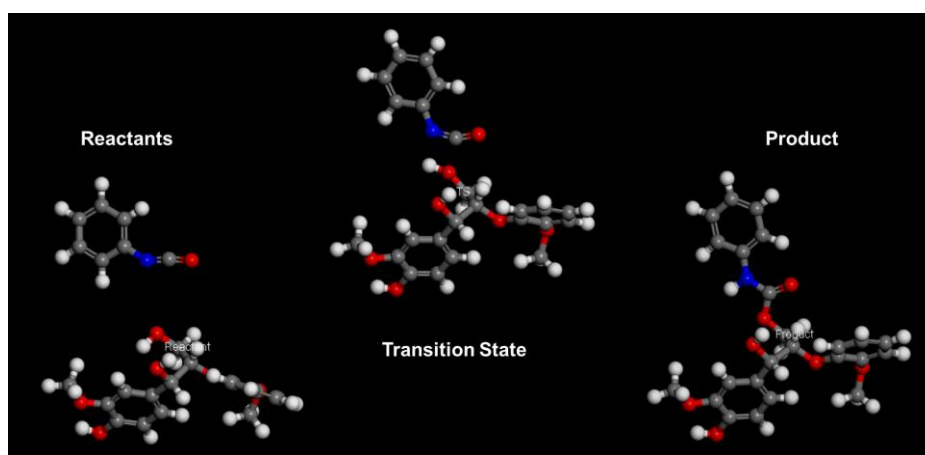


Figure 12. Reaction trajectory document showing phenyl isocyanate reacting with a lignin model compound

Figure 12 demonstrates the geometry of the transition state for the reaction between a lignin model compound and phenyl isocyanate. The transition state is a four atom complex, evolving from a hydrogen bond between the nitrogen of the isocyanate and the hydrogen on the hydroxy group, while the oxygen of the hydroxy group performs a nucleophilic attack on the carbon in the isocyanate group. This structure is very close to the one demonstrated by other computational studies.^{84,98} In fact, the computed energy barrier for the methanol-phenyl isocyanate reaction (130 kJ/mol) was very close to that of a computational study from literature (128 kJ/mol),⁸⁴ indicating that the developed model can reasonably predict activation energies for the urethane formation reaction.

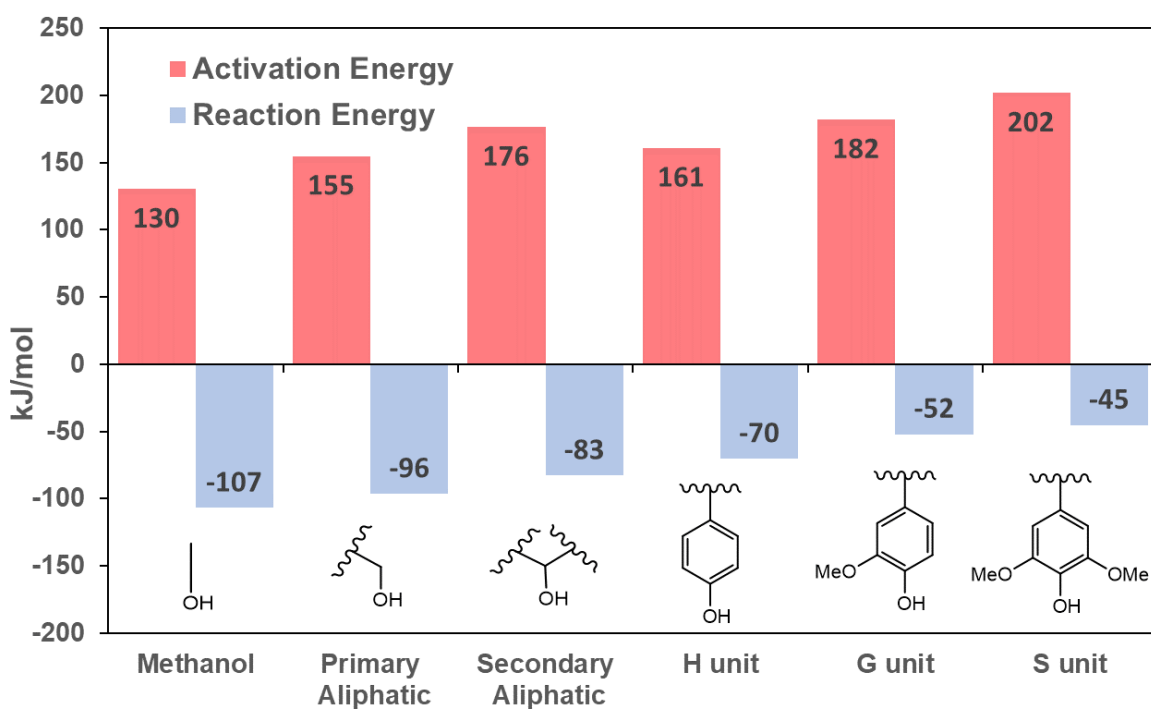


Figure 13. Reaction energy and activation energy for reactions of lignin model compounds with phenyl isocyanate

The results of the transition state searches generally matched expectations. Experimental studies have shown that lignin OH groups' reactivity towards isocyanates is in the order aliphatic

> H > G > S.^{52,99} According to kinetic theory, the reaction rate is inversely proportional to the activation energy by the Arrhenius law; thus, one would expect that the activation energy barrier for the hydroxy-isocyanate reaction follows the trend methanol < aliphatic < H < G < S. This is generally observed, and the addition of methoxy groups to the phenolic ring of lignin appears to significantly increase the activation energy. Simultaneously, the reaction energy (ΔE_{rxn}) showed the opposite trend, which indicates that the steric hindrance of the lignin molecules makes urethane linkages less thermodynamically stable. Interestingly, secondary aliphatic hydroxy groups show a much higher activation energy compared to aliphatic primary hydroxy groups; in fact, the activation energy for the reaction at secondary aliphatic hydroxy groups is higher than that for phenolic H-units. This could be because the additional steric hindrance of the lignin molecule near the secondary hydroxy groups negates the less nucleophilic nature of the OH group on the phenolic H-unit. If anything, the data collected here suggests that lignin varieties with a greater amount of H units, which are mainly found in herbaceous plants, would be best suited for PU applications that require a high crosslinking density between lignin and isocyanates.

Currently, no other computational study has attempted to model the reaction profile of lignin with isocyanates. Overall, these simulations are a good first step towards modeling the activation energy of the urethane formation reaction in lignin, but they need to be further optimized, and computed at a higher level of theory (using hybrid orbitals), to accurately model the system. Additionally, the clearly higher activation energies of G and S units provide motivation for developing lignin polyols through oxyalkylation with propylene carbonate, which will replace the sterically hindered S and G units in lignin with secondary aliphatic hydroxy groups.

3.2 Comparative Analysis of Lignin Polyols

Eleven different lignin varieties were used to synthesize lignin polyols, and their properties, including molecular weights, viscosity, and hydroxy contents were measured. The properties of the synthesized lignin polyols are shown in tables 6 and 7. Overall, this study showed that the OH values of the lignin polyols were relatively similar; in fact, analysis of variance between the organosolv and kraft pulping methods showed that the OHV of the polyols did not significantly vary between isolation processes ($p > 0.05$).

Table 6. Properties of eleven different lignin polyols

Lignin ID	Sources	Processing	Lignin OH Value (mg KOH/g)	Lignin Polyol OH Value (mg KOH/g)	Lignin Polyol Viscosity (cP)	Unreacted PC Content of Polyol (wt%)
1-K-SW	Softwood	Kraft	324	102	42	78
2-O-SW	Softwood	Organosolv	231	82	60	74
3-O-HW	Hardwood	Organosolv	274	96	17	78
4-O-CS	Corn Stover	Organosolv	218	85	27	79
5-S-WS	Wheat Straw	Soda	306	87	26	81
6-K-HW	Hardwood	Kraft	332	99	22	80
7-S-HW	Hardwood	Soda	368	80	12	85
8-O-WS	Wheat Straw	Organosolv	198	96	324	66
9-K-HW	Hardwood	Kraft	374	98	10	84
10-K-	Softwood	Kraft	261	123	93	74
11-O-	Wheat Straw	Organosolv	209	114	71	75

The main observation from this experiment was that only a small amount of propylene carbonate was actually grafted onto the lignins to make lignin polyols; unreacted PC measurements indicated that 66-85 wt% of the propylene carbonate remained in solution, resulting in a relatively low viscosity. Additionally, there was a correlation (Pearson's $r = 0.80$)

between lignin hydroxy content and unreacted PC content; this is unsurprising as the amount of PC added was stoichiometrically balanced with the lignin hydroxy content. As a result, the remaining experiments using these lignin polyols significantly reduced the amount of propylene carbonate used in the synthesis of lignin polyols, from a 1:10 lignin OH:PC molar ratio to a 1:5 molar ratio.

Table 7. Molecular weight distributions of lignins and liquid lignin polyols

Lignin ID	Unmodified Lignin Mn (Da)	Lignin Mw (Da)	Lignin Dispersity	Lignin Polyol Mn (Da)	Lignin Polyol Mw (Da)	Lignin Polyol Dispersity
1-K-SW	2002	7998	4	3590	13630	3.8
2-O-SW	1433	5758	4	2300	7540	3.3
3-O-HW	1555	4089	2.6	2440	9280	3.8
4-O-CS	2303	9348	4.1	2790	11240	4
5-S-WS	1607	4458	2.8	3110	11700	3.8
6-K-HW	2676	12554	4.7	5440	30130	5.5
7-S-HW	1844	6465	3.5	4980	20040	4
8-O-WS	1914	5409	2.8	3640	12980	3.6
9-K-HW	1344	3122	2.3	2560	7490	2.9
10-K-SW	1910	14670	7.7	5160	26410	5.1
11-O-WS	1800	4950	2.8	3080	8910	2.9

One interesting observation from the GPC data visible in Table 7 and Figure 14 is that lignins synthesized with the soda and kraft processes tended to have a higher conversion into high molecular weight fractions, compared to organosolv lignins. This can be attributed to a variety of reasons. In general, kraft and soda processes increase the amount of phenolic hydroxy groups in lignin by breaking aryl-ether linkages, resulting in more places for propylene carbonate to react with lignin. For instance, in this study, kraft and soda lignins had an average hydroxy content of 5.7 ± 0.9 mmol/g, compared to 4.0 ± 0.5 for organosolv lignins. Additionally, these

processes often leave elemental impurities like sodium which can catalyze the reaction between lignin and cyclic carbonates.¹⁰⁰ Additionally, it is possible that some of the lignin molecules formed crosslinked with each other through carbonate linkages, increasing weight average molecular weight and dispersity. Such a reaction was also reported by Kuhnel et al.⁷² This crosslinking reaction occurs at lignin's hydroxy groups, so it is likely that kraft and soda lignins, with higher hydroxy contents than organosolv lignins, would experience more of this crosslinking side reaction, leading to higher molecular weights and dispersities.

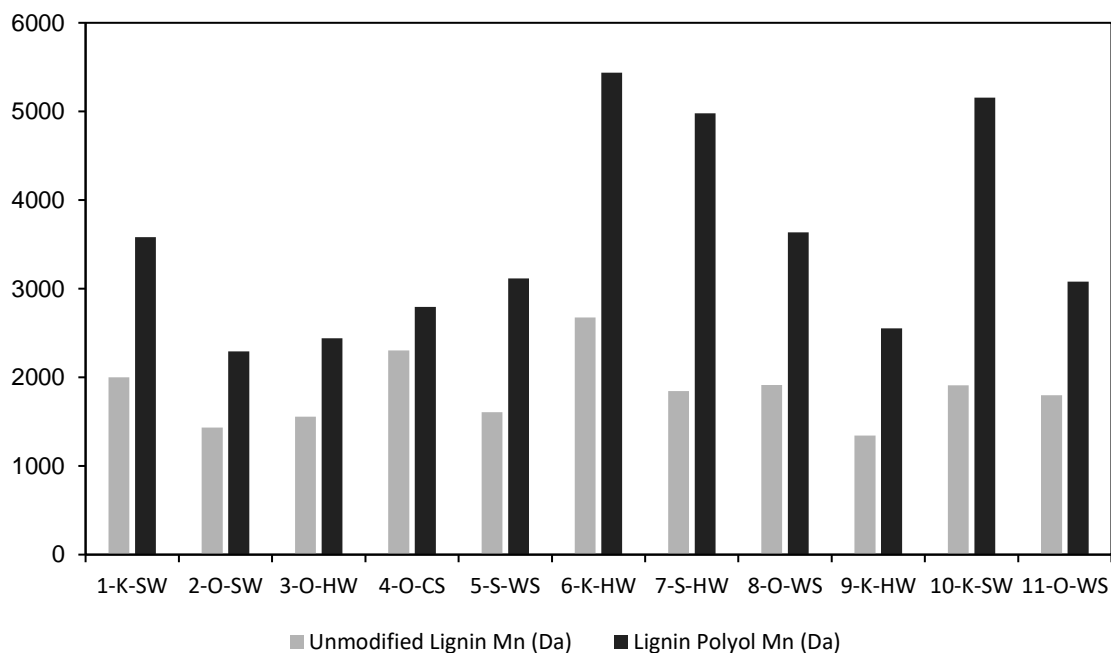


Figure 14. Comparison of molecular weight (Mn) before and after lignin oxypropylation

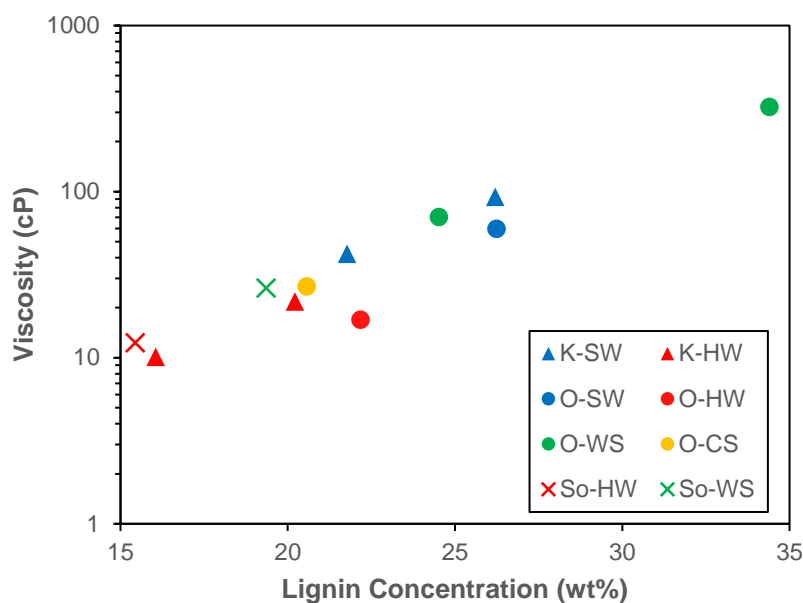


Figure 15. Polyol viscosity vs lignin concentration of lignin polyols

Figure 15 shows that the lignin concentration (inverse of unreacted PC content) has an excellent correlation ($p = 0.89$) with polyol viscosity. However, there were no clear correlations between lignin polyol viscosity and molecular weight. This is likely because there was a large difference in lignin concentrations in each polyol. For instance, the organosolv lignins tended to have higher viscosities because they have a lower hydroxy value, and thus used less propylene carbonate to react with each lignin hydroxy group. Future studies could prepare lignin polyols at various concentrations and use GPD data to fit Mark-Houwink parameters to the lignin polyols and obtain a better understanding of each lignin polyols macromolecular structure.

3.3 Flexible PU Foams Synthesized with Lignin Polyols

The computational study and comparative analysis of lignin polyols respectively provided insights into the nature of lignin-based PUs and PC-oxypropylated lignin. The remainder of this project is focused on applying the developed lignin polyols into flexible PU foam formulations. To that end, three different lignins, each from a different biomass source and

isolation process, were used to make liquid lignin polyols that subsequently replaced up to 30 wt% of the petroleum-based polyol portion of a flexible foam formulation. One goal of this project was to use these foams in automotive seating applications, and the mechanical properties of these foams were compared to standards listed for automotive upholstery.

3.3.1 Lignin Properties

Table 8. Properties of lignins used for flexible polyurethane foam synthesis

Lignin ID	O-WS	K-SW	H-HW
Source	Wheat Straw	Softwood	Hardwood
Isolation Method	Organosolv	Kraft	Acid
Ash Content (wt%)	0.2	1.9	2.3
Na (ppm)	0.01	0.49	0.56
M _n (Da)	1580	1910	1110
M _w (Da)	6240	14670	5480
Dispersity	4	7.7	4.9
T _g (°C)	163	161	166
Aliphatic OH Content (mmol/g)	1.82	1.65	2.66
Condensed Phenolic OH (mmol/g)	0.13	0.59	0.43
Syringyl OH Content (mmol/g)	0.54	-	1.46
Guaiacyl OH Content (mmol/g)	0.74	1.64	0.48
Hydroxyphenyl OH (mmol/g)	0.32	0.18	0.12
Carboxylic Acid OH (mmol/g)	0.35	0.6	0.28
Total OH Content (mmol/g)	3.9	4.66	5.43
OH Functionality (f)	6.2	8.9	6.0

Table 8 shows basic compositional properties of the lignins used in this study. The organosolv-wheat straw (O-WS) lignin showed a much lower ash and sodium content compared to the kraft-softwood (K-SW) and hydrolysis-hardwood (H-HW) lignins, which is expected as

organic solvents are less likely to dissolve inorganic minerals.⁶² While all lignins displayed a similar glass transition temperature, there were significant differences in molecular weight, with the K-SW having the highest M_n and M_w , followed by the O-WS lignin and H-HW lignin.

Table 8 also displays the hydroxy contents of the lignins used in this study. As expected, the O-WS lignin has H, G, and S moieties, while the K-SW consists mainly of guaiacyl groups, and while the H-HW lignin is rich in syringyl units, but has comparatively few G units and only a few H units.^{93,101} Overall, the O-WS lignin had the lowest total hydroxy content, which might indicate that it would be well suited to flexible foams the lower OH value would result in a lower crosslinking density⁵⁴

The ³¹P-NMR spectra of the lignin polyols shows that the phenolic OH groups in K-SW lignins were completely converted to aliphatic OH groups, represented by the broad peak at 145.5-146.2 ppm. However, it should be noted the O-WS lignin polyols showed some residual phenolic hydroxy moieties, indicating that longer reaction times are required to achieve complete conversion (see Figure 16). This could inhibit foam performance, as isocyanates will preferentially react with aliphatic isocyanates. Additionally, several narrow peaks occur in the aliphatic OH region of the ³¹P-NMR spectra. These are likely glycols, such as propylene glycol that formed from side reactions as the reaction progressed.^{72,77,102} These glycols will generally act as a chain extender in PU foams, extending the length of the hard segment, and affecting the degree of phase separation within the cured polymer.¹⁰³⁻¹⁰⁵ Thus, the liquid lignin polyol is actually a mixture of PC-modified lignin, low molecular weight glycols, PC-oligomers, and excess PC acting as solvent.⁸¹ These spectra were then integrated to compute the total hydroxy content and hydroxyl value (OHV) of the polyols, shown in Table 9. As shown, the polyol total OH value generally corresponds with the total hydroxy content of the unmodified lignin.

3.3.2 Lignin Polyol Properties

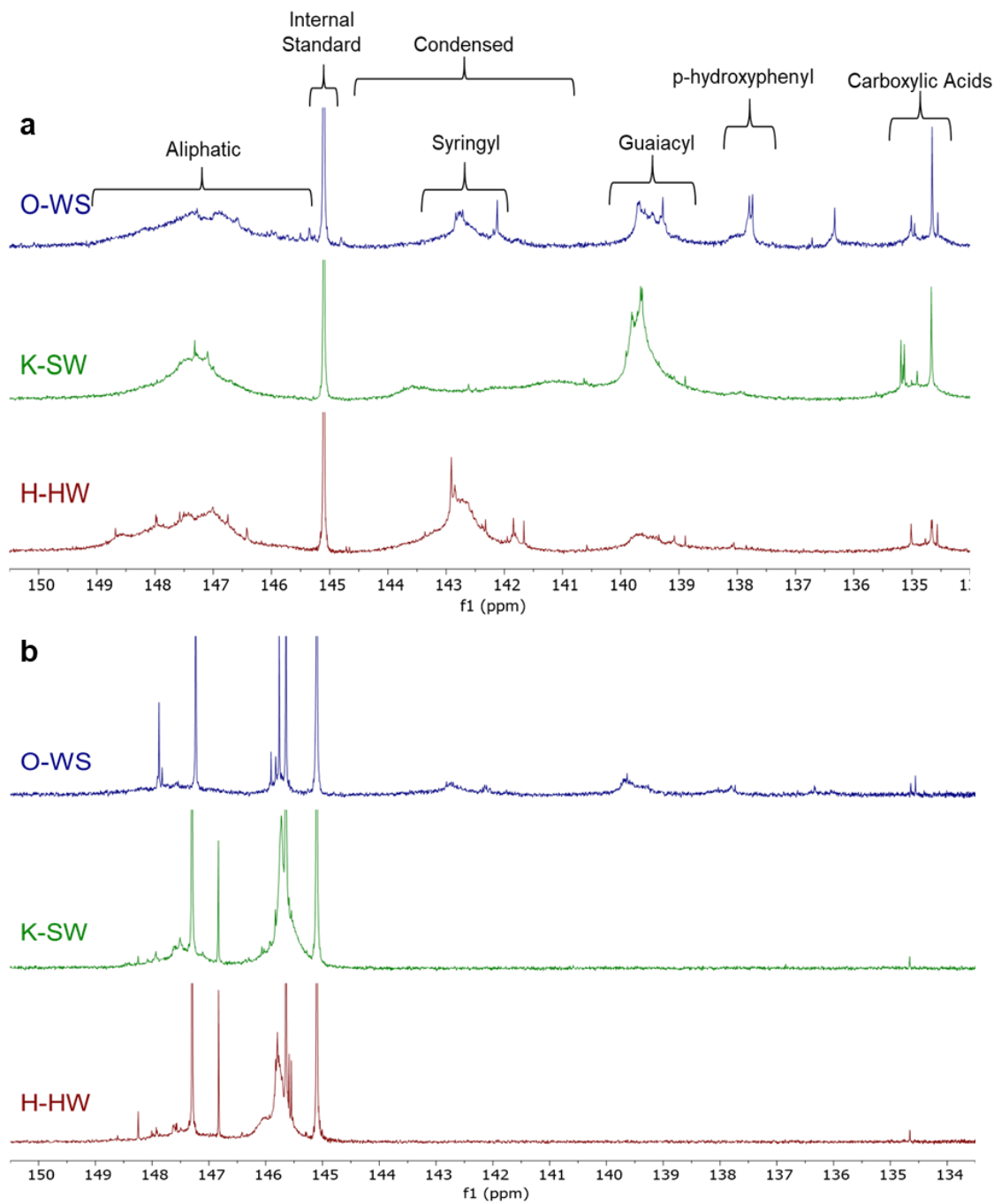


Figure 16. Phosphorous-31 (^{31}P NMR) spectra: a) Unmodified lignins. b) Lignin Polyols. Key:

O-WS: Organosolv-Wheat Straw, K-SW: Kraft Softwood, H-HW: Acid Hydrolysis-Hardwood

As the lignin-polyol screening study showed, the viscosity of a polymer solution will increase with concentration and molecular weight of lignin.¹⁰⁶ However, despite having a slightly higher unreacted PC content compared to the other lignin polyols, the K-SW lignin polyol had a much higher viscosity compared to the other lignins. This could be due to a variety of reasons, including the comparatively high molecular weight of the K-SW lignin or a high amount of side reactions that led to crosslinking of lignin and propylene carbonate oligomers via carbonate linkages.⁷² In contrast, the H-HW lignin polyol had a very low viscosity, which can be attributed to the low molecular weight of that lignin sample.

Table 9. Properties of synthesized lignin polyols

Lignin Used	Viscosity (cP) at 25 °C and 50 s⁻¹	OH Value (mg KOH/g)	Unreacted PC Content
O-WS	6000	105	53
K-SW	20000	142	62
H-HW	900	163	60

3.3.3 Foam Reaction Profile

Figure 17 shows how the addition of lignin polyol tends to catalyze the curing reaction of PU foams. The cream time of the foams, which corresponds to the beginning of gas nucleation in the reacting mixture, is slightly larger for the lignin containing foams; this could be attributed to the higher viscosity of lignin polyols which could impede visible bubbles from nucleating.¹⁰⁷

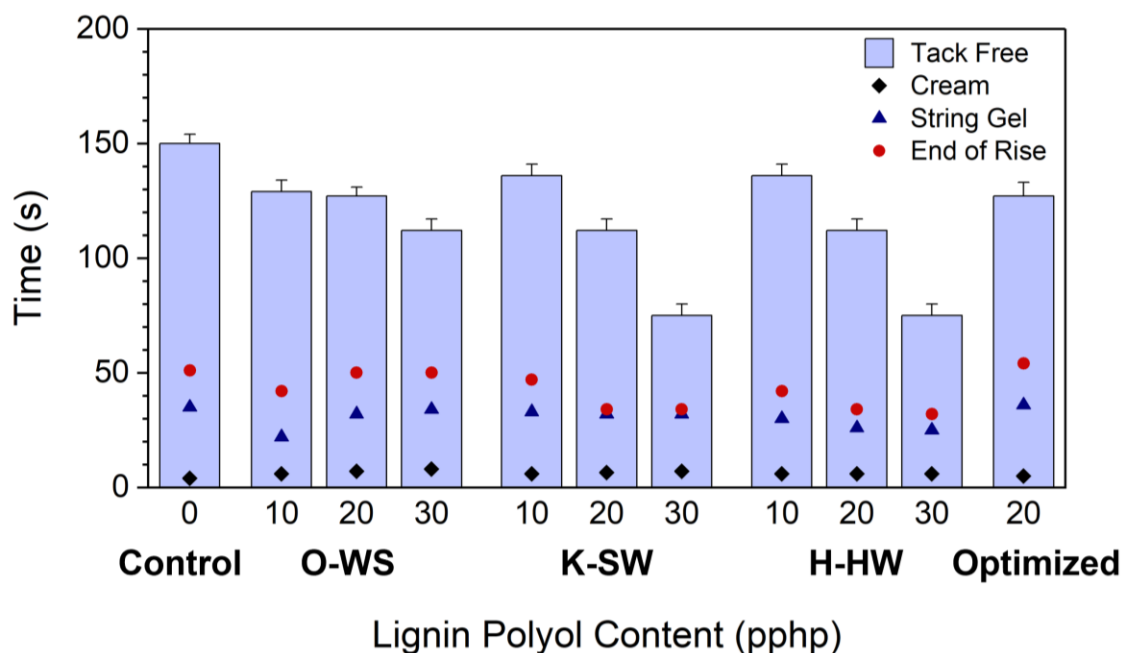


Figure 17. ASTM D7487 polyurethane foam cup test. Key: O-WS: Organosolv-Wheat Straw lignin; K-SW: Kraft-Softwood Lignin; H-HW: Acid Hydrolysis-Hardwood lignin. Control: Foam without lignin polyol, Optimized: Foam with 20 pphp K-SW lignin polyol and a reduced isocyanate index

The catalytic effect of the lignin polyols, which is made most evident by drastic reductions in the “tack-free” time as lignin polyol increased for the K-SW and H-HW lignins, can be attributed to the increased sodium content of those lignins and residual 1,8-Diazabicyclo(5.4.0)-undec-7-ene (DBU) catalyst remaining in the lignin polyol. In addition to catalyzing the reaction between lignin and cyclic carbonates, DBU is a highly effective catalyst of the polyol-isocyanate reaction,⁸⁴ causing a great reduction in reaction times with a high lignin-polyol content. Additionally, recent research by Maiuolo et al.¹⁰⁸ has indicated that sodium cations form a coordination structure with polyether polyols that catalyzes the reaction of polyols with isocyanates. Figure 16 showed that O-WS lignin polyol experienced incomplete conversion

of its phenolic hydroxy groups to aliphatic hydroxy groups. This reduced the O-WS lignin polyol's reactivity towards isocyanates, increasing reaction profile times.⁵²

3.3.4 *Scanning Electron Microscopy of Foams*

Scanning electron micrographs of the control foam, optimized foam, and foams synthesized foams with 30 pphp lignin polyol were taken to observe how liquid lignin polyol affects the morphology of PU foams. Using these low magnification images, ImageJ software was used to measure the average pore size of each foam, using 50 replicates per sample. The results in Table 10 indicate that at 30 pphp loading of lignin polyol, the pore size is much lower than in the control foam. This can be attributed to the higher crosslinking density of the foams made with lignin polyol (as all lignin polyols have a higher total hydroxy content than the polyether co-polyol), and the faster cure time of these foams, as evidenced by their reaction profiles, which could prevent cell opening from occurring before the foam fully cures.¹⁰⁹ In contrast, the optimized foam made with 20 pphp K-SW lignin polyol and a lower isocyanate index has a similar average pore size to the control formulation, which can be attributed to the slightly slower curing times due to the lower concentration of isocyanate. The decreased pore sizes can partially explain the higher moduli and reduced elongation to failure of the lignin-containing foams.

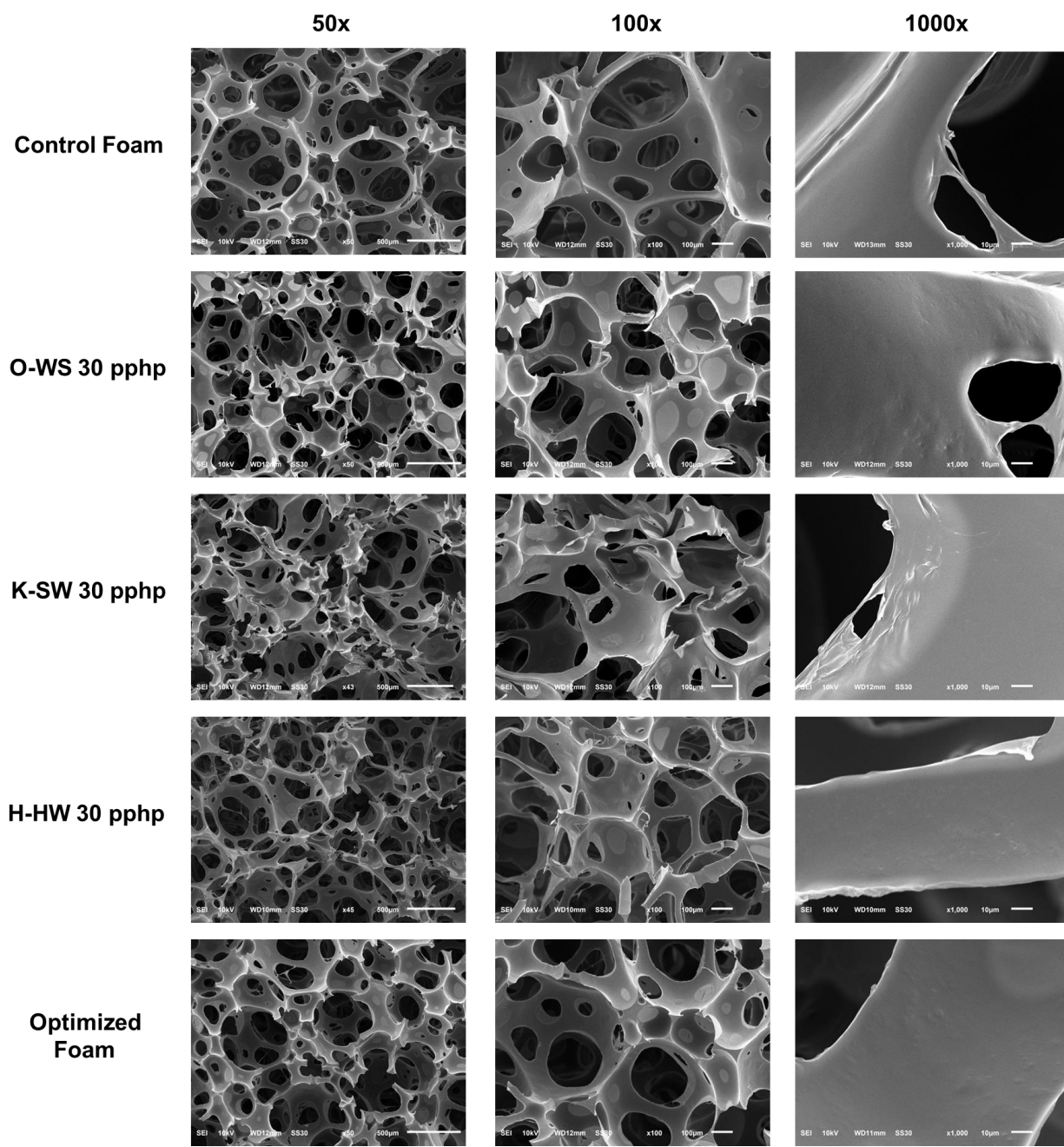


Figure 18. Scanning Electron Micrographs (SEM) of Synthesized Foams

Table 10. Average Pore Sizes of Flexible PU Foams

Foam Sample	Average Pore Size (μm)	Standard Deviation
Control	210	97
O-WS 30	151	64
K-SW 30	180	81
H-HW 30	180	79
Optimized (K-SW 20)	204	107

High magnification SEM micrographs at 100x and 1000x indicate that there are no agglomerated lignin particles in the PU matrix at a loading concentration of 30 pphp lignin polyol, and that the morphology of the foams is similar to the control. This indicates that lignin was successfully incorporated as a polyol into the foam matrix, and not as a filler particle, which often occurs when solid lignin powders mixed into a flexible foam mixture and can result in reduced mechanical properties.^{54,110}

3.3.5 Fourier-Transform Infrared Spectroscopy

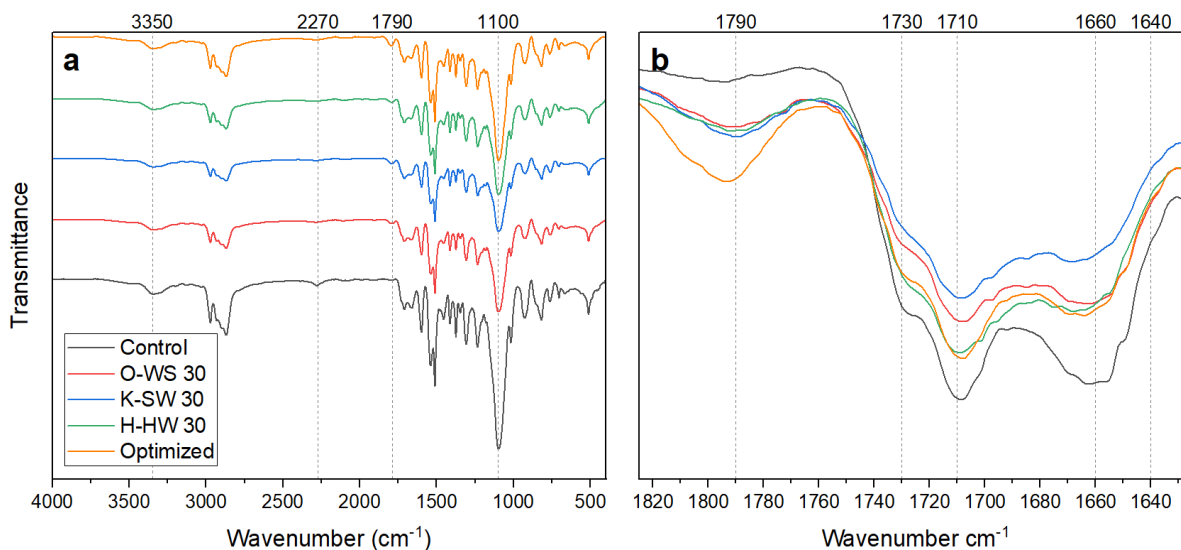


Figure 19. FTIR Spectra of selected polyurethane foams synthesized with 30 pphp lignin polyol:

(a) Full Spectra (b) Carbonyl stretching region

As Figure 19 shows, the infrared spectra of the foams made with 30 pphp lignin appear very similar to each other, but with slight differences compared to a foam made without lignin polyol. First, the isocyanate peak centered at 2270 cm⁻¹ is still visible in the control foam, but has completely disappeared in foams made with lignin polyol. This could be due to the more reactive nature of the lignin polyol, as evidenced by the foam's reaction profile, due to the presence of residual DBU catalyst within the lignin polyol, or alternatively due to glycols and other PC-oligomers with primary OH groups that quickly react with isocyanates. Furthermore, the lignin-containing foams have a reduced intensity in the C-H stretching region (3000-2840 cm⁻¹). Additionally, the carbonate linkages within the lignin polyol appear at a small peak at 1790 cm⁻¹. In PUs, the ratio of the carbonyl peak intensities at between 1710-1715 cm⁻¹ (free urea) and 1650-1700 cm⁻¹ (monodentate hydrogen bonded urea) can be used to interpret the degree of microphase separation in PUs.^{46,47} The diminished hydrogen bonded urea peaks in the samples

with 30 pphp lignin polyol, indicate that the lignin polyol disrupts the ordering of the hard domains, reducing the degree of microphase separation.¹¹¹ Microphase separation plays a critical role in determining the mechanical properties of PU materials; for instance, the tensile strength and toughness of PU elastomers can be greatly improved by high degrees of microphase separation.¹¹² All foams exhibited only weak signals at 1640 cm^{-1} , which indicates a lack of bidentate urea linkages, indicating that overall, hard domain ordering was limited for all foams. This could partly explain the limited elastomeric activity of the lignin-containing foams. Other studies of lignin-PU have indicated that lignin tends to disrupt the ordering of the hard domains.⁴⁶ It was more difficult to resolve the free urethane (1730 cm^{-1}) and hydrogen-bonded urethane ($1700\text{-}1705\text{ cm}^{-1}$) compared to the urea units, which can be attributed to the high water content used for synthesis of these foams compared to other studies.^{45,113}

3.3.6 Mechanical Properties of Foam

The following figures display the measured mechanical properties of the foams partially made with lignin polyols. The dotted red lines on the graphs indicate standard mechanical property ranges for automotive seating applications. Error bars represent one standard deviation.

The densities of the foams (Figure 20) were generally within the acceptable range for automotive seating applications of $40\text{-}65\text{ kg/m}^3$, but they tended to vary based on the type of lignin polyol used. Foams made with O-WS and H-HW showed higher densities compared to the foam without lignin. This can be attributed to the higher hydroxy content of the lignin polyol and the accelerated curing reaction which prevents adequate time for gas bubbles to expand in the polymer matrix. Interestingly, the foams made with K-SW lignin polyol showed a similar density to the control foam at loading percentages of 10 and 20 pphp, but with an increased density at 30 pphp loading; this could be due to partial foam collapse.

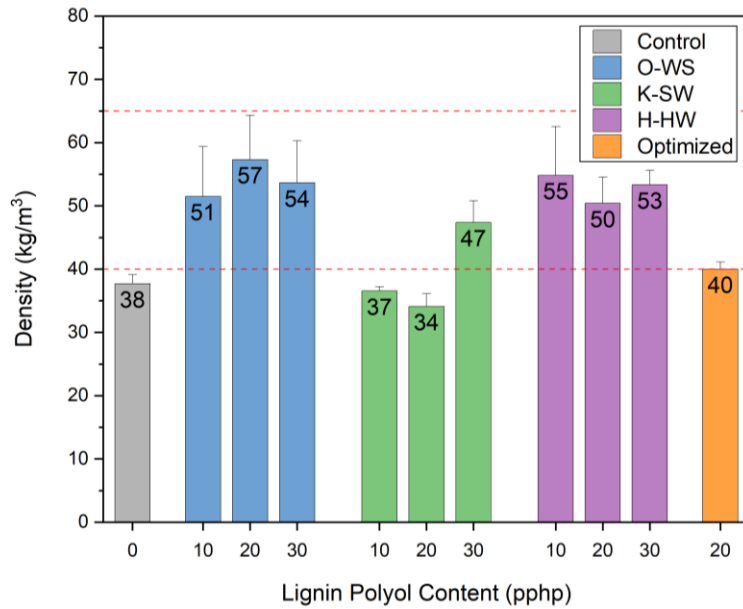


Figure 20. Apparent Densities of Flexible PU Foams synthesized with liquid lignin polyols. Key: O-WS: Organosolv-Wheat Straw lignin; K-SW: Kraft-Softwood Lignin; H-HW: Acid Hydrolysis-Hardwood lignin. Control: Foam without lignin polyol, Optimized: Foam with 20 pphp K-SW lignin polyol and a reduced isocyanate index

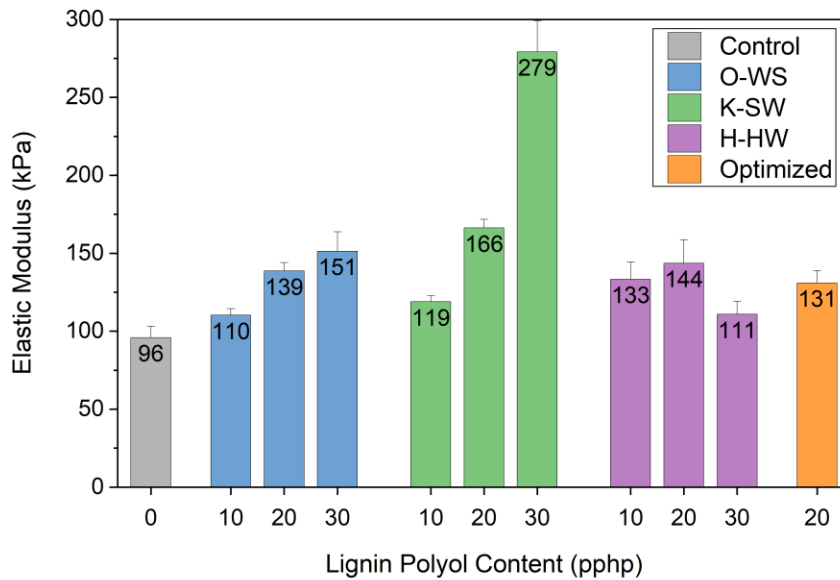


Figure 21. Elastic moduli, measured in tension, of flexible PU foams

Figures 21 and 22 summarize the results of tensile testing on the PU foams. The additions of O-WS and K-SW lignin polyol clearly increase the elastic modulus of the foams. This is expected, as lignin increases the hard segment content of the foams. Additionally, these lignins have a highly branched structure with many terminal OH groups which will increase the crosslinking density of the foams. Surprisingly, the foams synthesized with H-HW lignin polyol did not show this trend; the foam synthesized with 30 pphp H-HW lignin polyol actually had a lower elastic modulus compared to the foam synthesized with 20 pphp lignin polyol.

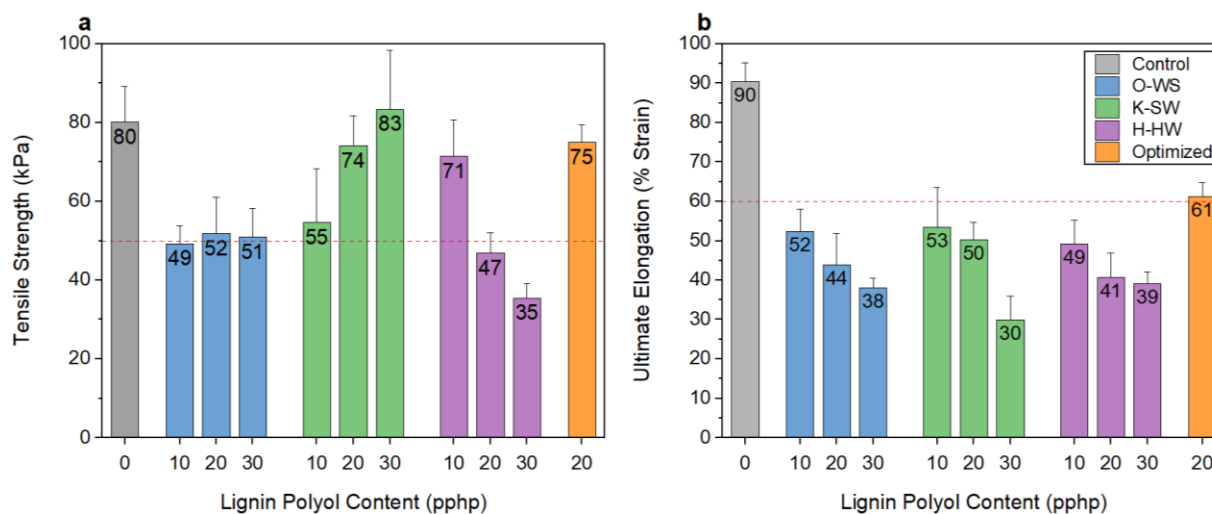


Figure 22. Tensile strength (a) and ultimate elongation (b) of flexible PU foams synthesized with liquid lignin polyols

Additionally, it is clear to see that the foams synthesized with lignin polyols had severely reduced ultimate elongations compared to the control sample. This in turn contributes to the lower tensile strengths of some lignin-based foams, as they fracture at lower strains. This can be attributed to multiple issues. First, because the hydroxy content of these lignin polyols (90-150 mg KOH/g) is higher than the long-chain polyether polyol used as a co-polyol (28 mg KOH/g), more isocyanate is used to obtain the same isocyanate index. This increases both the crosslinking

density of lignin, and increases the amount of hard segment present in the foam. As a result, the elastomeric activity of the soft segment is hindered by the addition of lignin polyol.

Notably, the K-SW lignin polyol produced foams with the highest tensile strengths and moduli. Reasons for the comparatively superior performance of the K-SW lignin are not entirely clear, and require further study. Previous studies have shown that for lignins of the same type, but fractionated to obtain different molecular weight distributions, intermediate molecular weights ($M_n = 900$) and lowest dispersities ($\mathcal{D} = 1.8$) produced the best tensile strength and elongation when directly incorporated into flexible foams.⁵⁷ A separate study of lignin-PU elastomers also indicated that lower molecular weight lignin resulted in higher moduli, strength, and elasticity.¹¹⁰ It is possible that the higher hydroxy functionality of the K-SW lignin ($f = 8.9$) resulted in a greater crosslinking density for the foams made with K-SW lignin polyol. Overall, this highlights the biggest challenge in using lignin in flexible PU foam formulations: lignin's rigid, highly branched structure means that it cannot fully replace the soft segment in PU foams. However, this also means that lignin can effectively replace some of the hard-segments in PU foams, requiring less isocyanate, which is petroleum-derived and considered a toxic substance. For instance, the optimized foam formulation was made with an isocyanate index of 70, and 20 pphp of the K-SW lignin polyol, whereas all the other foams had an isocyanate index of 80. The optimized foam had an ultimate elongation of 61%, matching the required flexibility for automotive seating applications while still maintaining a high tensile strength.

Figure 23 displays the results of compression force deflection (CFD) measurements. To run this test, rectangular foam samples were compressed to a certain strain level and left to relax for one minute, as shown in Figure 23d. The compression force deflection (CFD) was recorded as stress after one minute relaxation at 50% strain, while the support factor is this ratio of these

stresses at 65% strain and 25% strain. The CFD value is an important measure of load bearing ability. Additionally, CFD values have been shown to be linearly proportional to density,⁴⁶ and so Figure 23b, which shows CFD normalized by foam density, gives a better estimate of how the polymer matrix of the foam actually performs.

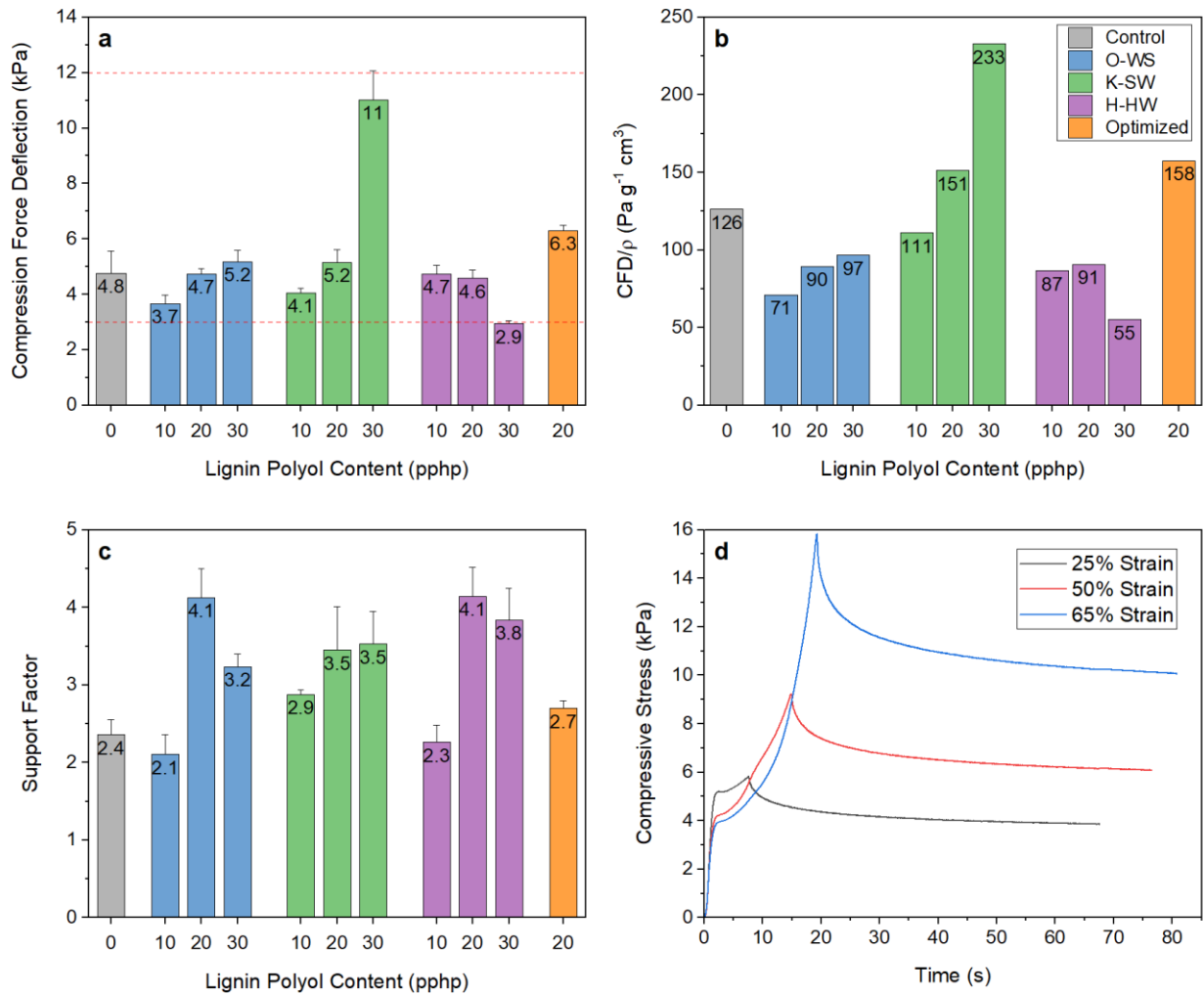


Figure 23. Compression testing results: a) Compression Force Deflection (CFD) values, b) Density-normalized CFD, c) Support Factor, d) Stress relaxation during a CFD test

The compressive properties indicate that the K-SW lignin polyol produces foams with the highest load-bearing properties, even when corrected for density. The higher hydroxyl functionality ($f = 8.9$) of K-SW lignin compared to that of O-WS ($f = 6.2$) and H-HW ($f = 6.0$),

and the polyether polyol ($f = 3$) could result in more urethane crosslinks per lignin molecule, increasing the crosslinking density of the foams and resulting in better load bearing properties. As discussed earlier, the O-WS lignin polyol had some residual aromatic hydroxyl groups that did not react with propylene carbonate, leaving it with phenolic hydroxy groups that are less reactive towards isocyanates; this could explain its worse load-bearing properties compared to the K-SW foam. The H-HW lignin polyols produced foams with particularly poor compressive properties, with CFD values lower than those of the control foam. This is surprising, given lignin's rigid structure and the H-HW lignin's high hydroxyl content; one would expect it to provide more load bearing compared to the control foam. One hypothesis for the poor mechanical properties of this foam are its high residual sugar content and low molecular weight.

Additionally, it was generally observed that addition of lignin to the foams increased the support factor. This empirical parameter is related to the compression modulus, but is also widely used by industry to measure how much cushioning a piece of foam would provide. For instance, a foam cushion with higher support factors would be less likely to "bottom out" when someone sits on it.¹¹⁴ Thus, lignin can play a critical role in improving foam performance in seating applications.

The tear strength corresponds to the maximum force required to propagate a tear through the foam; it is analogous to the fracture toughness of a bulk material, and serves as an empirical measurement of foam durability in real-world applications. A foam with high tear strength would ideally have both high tensile strength and elongation at break.

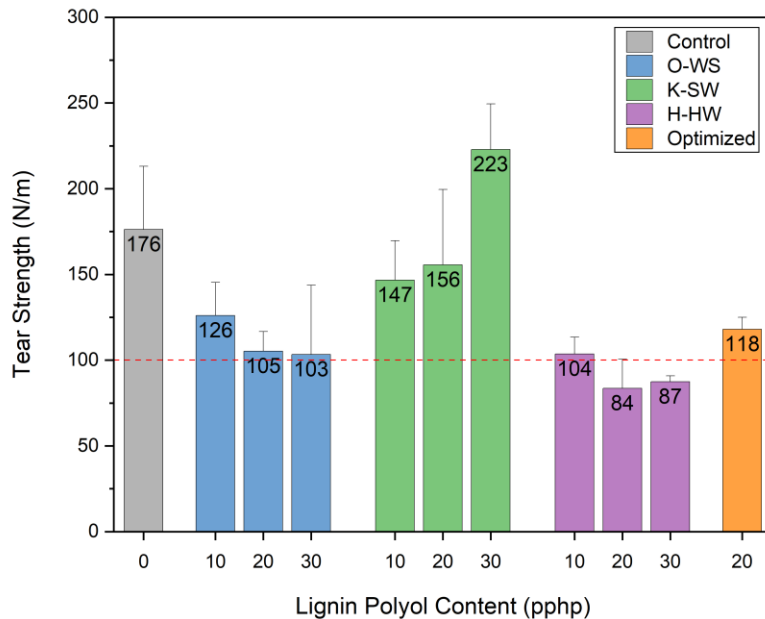


Figure 24. Tear strength of flexible PU foams made with liquid lignin polyols

The tear strength shows a similar trend to the other mechanical properties, in that the foams made with K-SW lignin polyol clearly outperform those made with the O-WS and H-HW lignin polyols. In fact, with addition of K-SW lignin polyol, the tear strength showed an increasing trend, while addition of O-WS and H-HW lignin polyols showed a decreasing trend in tear strength. All foams made with the K-SW lignin polyol met the minimum 100 N/m standard required for automotive seating applications.

The “optimized” foam demonstrated that a foam with 20% of its petroleum polyol portion replaced with a K-SW lignin polyol can meet the standard mechanical property requirements for automotive seating application, with a reduction in the isocyanate index. Because isocyanates are toxic and volatile petroleum-derived materials, this has the added bonus of increasingly the sustainability of the final foam. The optimized foam had a low density, a comparable tear strength to the control foam, and a noticeably improved ultimate elongation compared to the other lignin-based foams. However, it should be noted that tear strength

decreased significantly when the isocyanate index was reduced, although it still met the minimum 100 N/m required for automotive seating applications. Thus, while reducing the isocyanate index can be an effective method for improving the flexibility and bio-based content of lignin-based PU foams, it can also negatively affect some critical performance parameters.¹¹⁵

3.3.7 Thermogravimetric Analysis

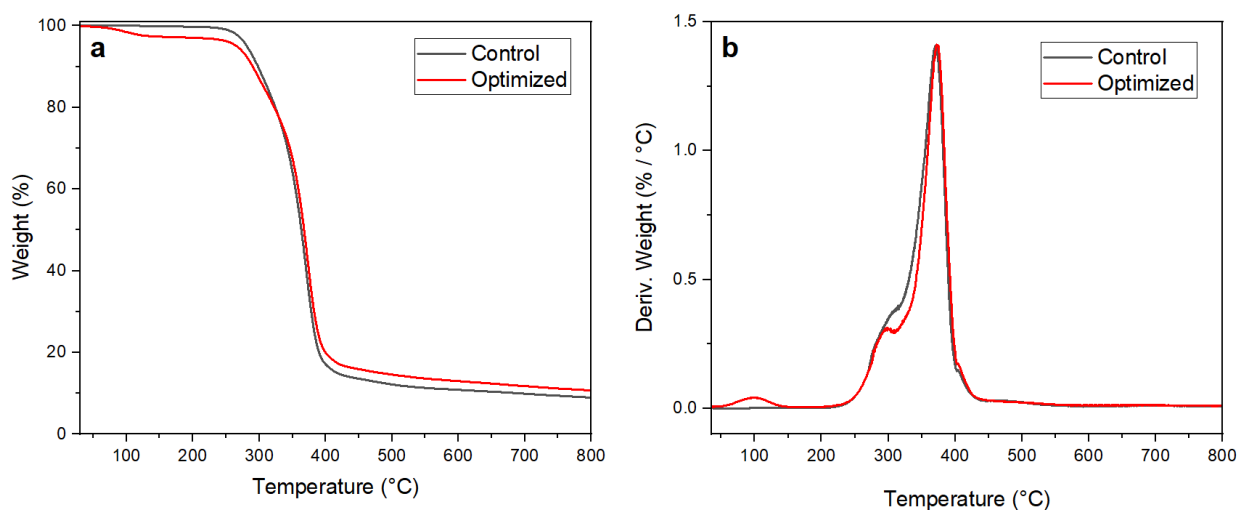


Figure 25. Thermogravimetric analysis of flexible PU foams in nitrogen. a) Weight loss thermogram. b) Derivative of weight loss. Key: Control: Foam made with 0 pphp lignin polyol. Optimized: Foam made 20 pphp K-SW lignin polyol and an NCO Index of 70

Thermogravimetric analysis (Figure 25) of the synthesized foams revealed that foams with lignin polyols exhibited about 5% weight loss from 100-200 °C. This can be attributed to evaporation of small molecules of unreacted PC and PC-oligomers (formed as side-products during polyol production) that did not react with lignin or isocyanates and were not incorporated into the polymer matrix.¹¹⁶ At 250 °C, irreversible degradation of the urethane linkage begins, peaking at a shoulder around 313 °C; interestingly, the lignin-containing foam appears to have a more well defined shoulder peak at 310 °C compared to the control foam. The polyol soft

segment of the foams then pyrolyzes near 370 °C. Additionally, the lignin containing foams all generated more residual char following degradation of the urethane linkage and pyrolysis of the polyols; this can be attributed to the more complex molecular structure of the lignin which is more difficult to volatilize.

3.3.8 Dynamic Mechanical Analysis

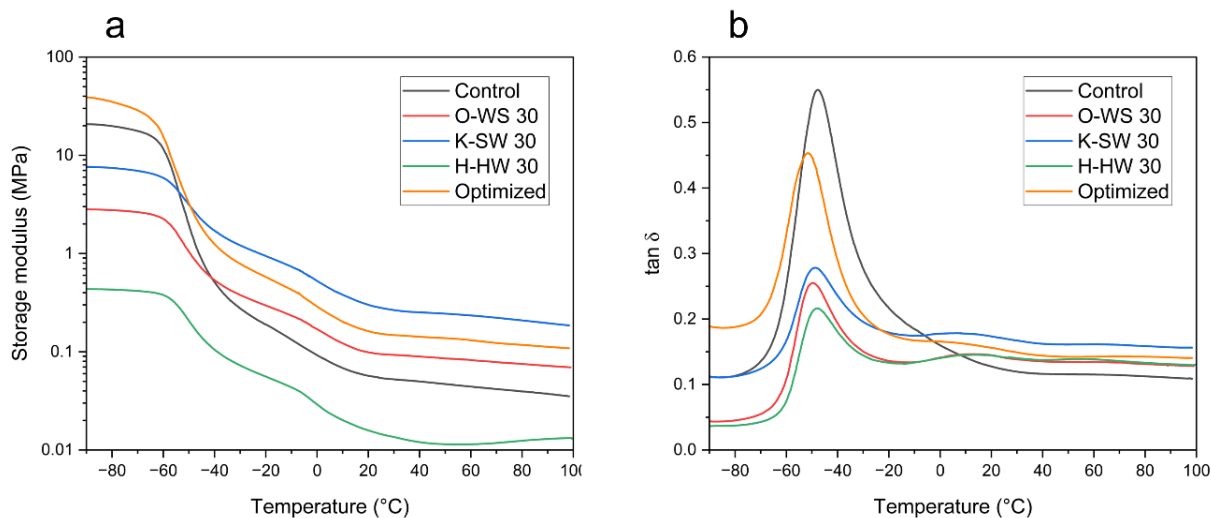


Figure 26. Dynamic mechanical analysis (DMA) of foams, collected at 1 Hz: a) Storage modulus and b) $\tan \delta$ between -90 to 100°C

Despite the large amount of noise present in the data, which can largely be attributed to the low moduli of the foams compared to bulk materials, DMA analysis of the foams (Figure 26) is very revealing with regard to mechanical properties. Below T_g , the control foam had a higher storage moduli than all foams with 30 pphp lignin. This result is somewhat surprising, especially because the control foam had a lower density than the other measured samples, and can be potentially attributed to the closer packing among soft-segments in the glassy state, compared to the highly branched lignin structure. DMA studies on bio-based rigid PU foams indicated that higher degrees of phase separation tend result in higher storage moduli in the glassy state.¹¹⁷

FTIR spectra (Figure 19) of these foams indicated that the control foam had a higher degree of phase separation than the lignin-containing foams, which could explain why the control foam had a higher storage modulus in the glassy state compared to the foams made with 30 pphp lignin polyol. Above T_g , the O-WS and K-SW based foams showed a clearly higher storage modulus than the control foam, which can be attributed to the aromatic structure of the lignin backbone, and a greater crosslinking density among the lignin-containing foams.

Table 11. Soft-segment glass transition temperature of synthesized foams, as measured by DMA

Foam	T_g (C)
Control	-47.8
O-WS 30	-49.6
K-SW 30	-48.8
H-HW 30	-47.7
Optimized	-51.7

Additionally, the collected DMA data shows that the soft-phase glass transition is lower in most of the lignin based foams. This is surprising, because a previous study on lignin-based flexible foams, which contained 6.7 wt% soda-herbaceous lignin modified with propylene oxide, used DMA to show that lignin either does not affect the soft-segment glass transition temperature, or partially mixes with soft-segment molecules and slightly increases the T_g .⁴⁵ The surprising decrease in T_g seen in these foams can be attributed to the presence of residual propylene carbonate, which acts as a plasticizer, reducing the glass transition temperature and making the foam more flexible.²⁰ Finally, the optimized foam, which has a higher proportion of soft segment because it only contains 20 pphp lignin polyol and has a lower isocyanate index,

shows a higher intensity $\tan \delta$ peak at the soft phase transition, as well as a higher storage modulus than the control foam both above and below T_g .

3.4 Partial-Least Squares Regression Modeling

A partial least squares regression model was developed to better understand relationships between lignin, lignin polyol, and foam properties. Lignin and polyol properties serve as the predictor variables, while the foams' mechanical properties are the response variables. Figure 27 shows that the fitting accuracy of this model is about $R^2 = 0.78$, while the prediction ability (Q^2) is about 0.69). For a small model with only 10 samples, this is a low, but acceptable level of fitting.

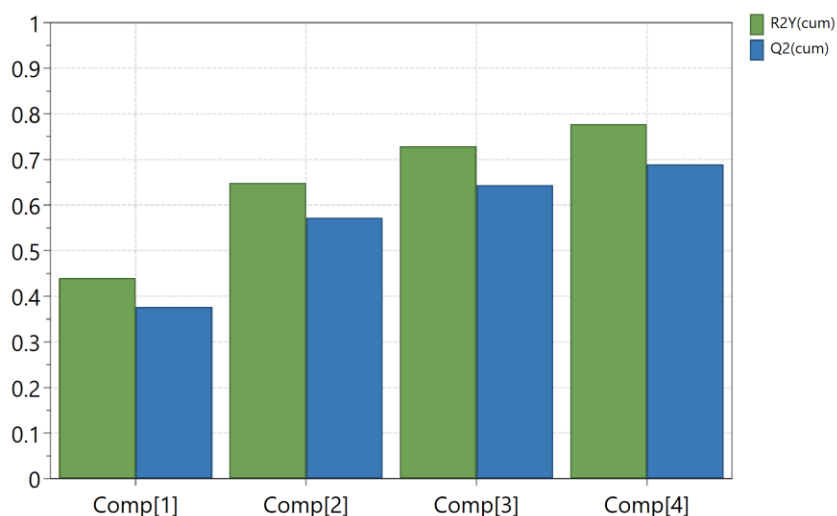


Figure 27. Cumulative fitting accuracy (R^2Y) and prediction ability (Q^2) of the PLS-R model

The PLS-R loadings plot in Figure 28 clarifies several relationships between lignin properties, foam synthesis parameters, and the properties of the flexible PU foams. Loadings plots allow easy interpretation of correlations between variables in a large data set. Predictor and response variables that are near each other and towards the edge of the plot will be strongly correlated. Variables that are highly negatively correlated will appear on opposite sides of the

graph with respect to the origin, while variables that tend to not be relevant will be plotted near the origin of the graph.

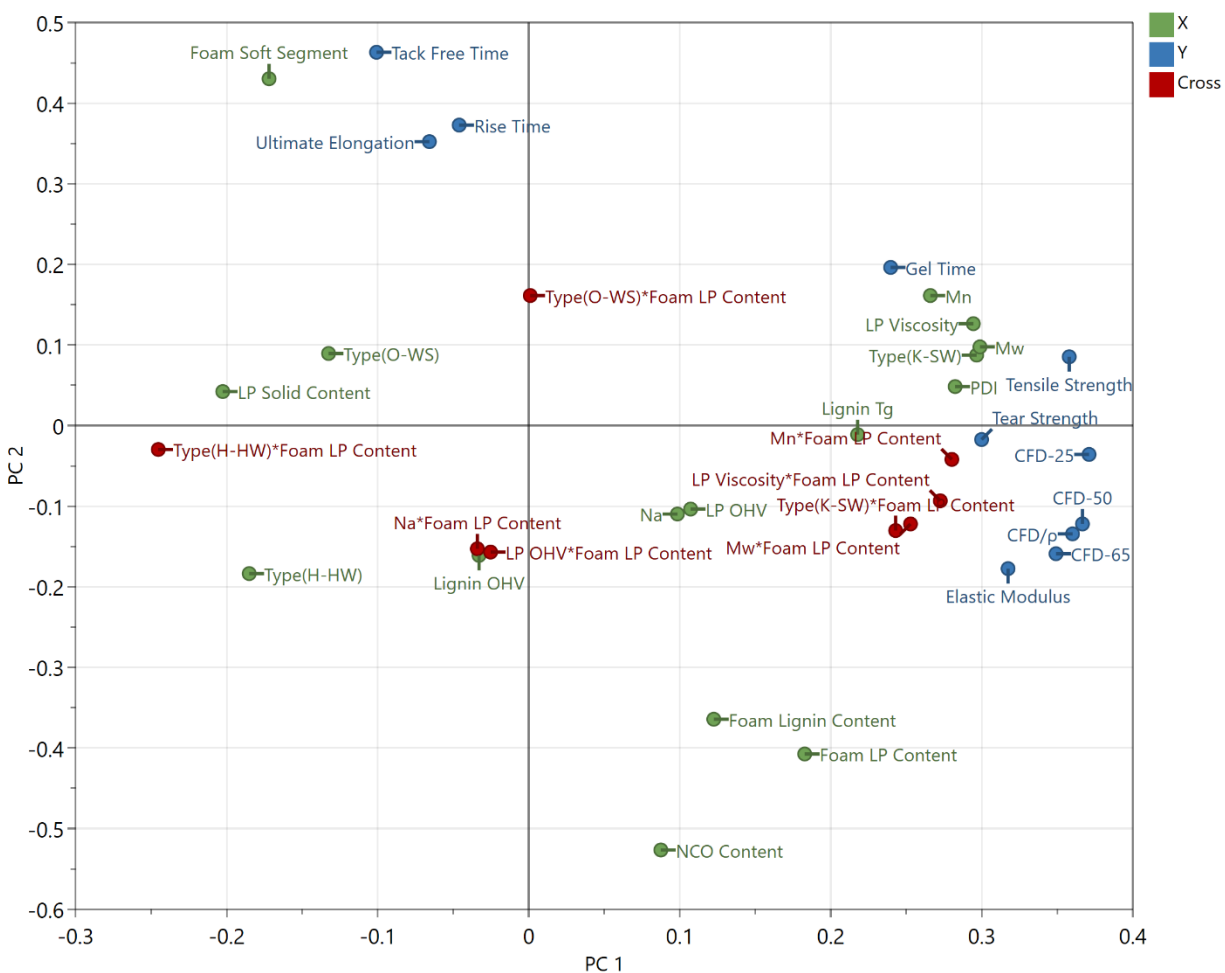


Figure 28. Partial Least Squares Regression (PLS-R) loadings plot

As expected, one of the strongest predictors of foam properties was the NCO content (by wt%) of the foams. While the synthesized foams were stoichiometrically balanced to have an isocyanate index of 80, the actual amount of isocyanate in the foam increased with lignin polyols that had higher hydroxy value. This can affect several of foam properties by increasing the foam crosslinking density and the amount of hard domains within the foam microstructure, leading to higher elastic moduli and load bearing properties. Additionally, Figure 28 shows that NCO

content is highly negatively correlated with the end-of-rise and tack-free time of the foams. This was not immediately apparent in the original dataset, but can be rationalized that the higher concentration of NCO and OH groups in the reacting foam mixture will result in faster reaction rates, decreasing the rise and tack free times. M_n , M_w , and viscosity, when crossed (multiplied) with lignin-polyol (LP) content, appeared to be decently correlated with the tensile strength and load-bearing properties of the foams, suggesting that for flexible foams, lignin polyols synthesized with higher molecular weight lignins tend to improve mechanical properties. However, because only three lignins were used in this study, this relationship cannot be stated definitively and requires additional study.

CHAPTER 4 Conclusions and Future Work

4.1 Conclusions

Lignin is the most abundant aromatic polymer and is produced as a byproduct of chemical pulping and biorefineries. Currently, lignin is mostly burned to produce energy for those plants, but it can be easily extracted from pulping liquor and be used as a feedstock in bio-based products, in which it acts as a carbon sink. Because lignin is a natural polyol, there have been extended efforts to incorporate it into polyurethane (PU) materials. That said, there have been relatively few studies on using lignin as a polyol in flexible PU foam formulations. This thesis discussed efforts to develop flexible PU foams using lignin as a natural polyol to partially replace petrochemical polyols.

First, it was shown that density functional theory (DFT) modeling can be used as a tool for evaluating lignin-based PU systems. Lignin's structure contains a variety of aliphatic and phenolic hydroxyl (OH) groups with different electronic environments. These phenolic hydroxy groups are further divided into *p*-hydroxyphenyl (H), guaiacyl (G), and syringyl (S), that respectively have 0, 1, and 2 methoxy units at the ortho position of their phenolic rings. Transition state searches executed using Dmol³ indicated that the activation energy for reactions between lignin model compounds and phenyl isocyanate changed significantly based on the type of lignin hydroxy functional groups that reacted with phenyl isocyanate. Specifically, it was observed that the computed activation energy increased in the order primary aliphatic < H-unit < secondary aliphatic < G-unit < S-unit. Furthermore, this result indicated that lignins with higher amounts of H-units, which are mainly found in herbaceous plants, would be well suited for PU applications. Additionally, these findings serve as a motivation for oxyalkylating lignin with propylene carbonate (PC), because this process converts lignin's phenolic hydroxy groups to

aliphatic hydroxy groups. Thus, oxyalkylating lignin with PC will result in lower activation energies, much faster reaction times and higher crosslinking densities when these lignins are incorporated into PU materials.

On a more general level, this study demonstrated the effectiveness of using computational chemistry to model lignin-PU systems; the results collected generally correlated with experimentally observed data collected by earlier studies. This indicates that density functional theory DFT can be applied to understand reaction kinetics in other lignin polymeric-based systems, including epoxies, and phenolic resins.

While there has been some success in using solid powdered lignin as a polyol in flexible PU foam formulations, previous studies have indicated that powdered lignin largely acts as a filler in PU foams, and most PU production facilities require liquid polyols. Thus, the remainder of this project focused on using propylene carbonate to oxyalkylate lignin to synthesize liquid lignin polyols for PU foam preparations. Propylene carbonate is a green solvent, which is non-toxic, VOC-exempt, and can be produced by the uptake of carbon dioxide, a greenhouse gas. Thus, unlike other lignin-based technologies that use toxic petroleum-derived propylene and ethylene oxide to develop lignin polyols, this process is significantly greener and more sustainable.

First, eleven different lignins were used to synthesize lignin polyols, using a 1:10 molar ratio of lignin hydroxy groups to PC molecules. It was observed that the OH values of these polyols were not significantly different, and all were in the range of 80-120 mg KOH/g. Since the ratio of lignin to PC was very high (1:10), the lignin-polyol samples had shown similar viscosity ranging from 10-300 cP. This is due to the high amount of unreacted PC acting as a solvent. Molecular weight analysis of lignin-polyol samples showed a slight increase in

molecular weights, confirming grafting of PC to lignin. As a result, for the liquid lignin polyols used for foam synthesis, the molar ratio lignin hydroxy groups to PC was reduced to 1:5.

The last part of this study focused on using three different types of lignin to make lignin polyols and then incorporating them into flexible foams, such that 10-30% of the polyol portion was replaced with lignin-polyols. Liquid lignin polyols, using a 1:5 molar ratio of lignin OH groups to PC, were synthesized by oxyalkylating three lignins from different biomass sources (softwood, hardwood and wheat straw) and isolation processes (kraft, acid hydrolysis and organosolv). It was found that the addition of the lignin polyols to the foams accelerated the reaction of the polyols towards isocyanates, resulting in smaller cell sizes, likely due to the lignin's sodium content (acts as catalyst) and presence of residual 1,8-Diazabicyclo[5.4.0]undec-7-ene (DBU) catalyst in the lignin polyol solution. Future work thus should find methods to remove or neutralize the DBU catalyst from the polyol prior to foam synthesis, or lower the amount of other catalysts added to the foam formulation. Interestingly, the type of lignin used to make the polyols significantly affected the mechanical properties of the foams. Foams made with a Kraft-Softwood (K-SW) lignin polyol resulted in a stiffer foam with higher tensile strength and load-bearing properties compared to foams made with an Organosolv-Wheat Straw (O-WS) and Acid-Hydrolysis Hardwood (H-HW) lignin. This is likely due to the comparatively higher molecular weight and functionality of the Kraft-Softwood lignin than the other two lignins.

More advanced characterization methods elucidated how the lignin polyol affects the structure of the foam matrix. Interestingly, TGA analysis indicated that there was a small amount of propylene carbonate that remained in the foam. DMA suggested that the presence of this residual propylene carbonate acts as a plasticizer, resulting in a decrease of the soft segment glass transition temperature. Thus, while PC acts as an effective green solvent and

oxypropylation agent, further work will focus on removing the excess unreacted PC in the lignin polyol and substituting it with other bio-based co-polyols, which would further reduce the hydroxyl value of the lignin-polyol, while minimizing the plasticizing effect of propylene carbonate. Furthermore, FTIR analysis of the carbonyls peaks from 1640-1730 cm^{-1} suggested that the addition of lignin into the foam disrupted the hard-phase ordering and decreased the degree of microphase separation in the PU foam matrix, which can have adverse effects on foam mechanical properties.

Mechanical performance of foams made with 10-30 pphp lignin polyol and an isocyanate index of 80 showed that the addition of lignin polyol resulted in poor ultimate elongation. To increase the flexibility of the foams, an “optimized” foam formulation was created using 20 pphp of the Kraft-Softwood lignin polyol and a lower isocyanate index of 70. This optimized foam showed comparable density, load bearing performance, and tensile strength to those of a commercial polyether-based flexible foam. Moreover, the optimized foam with lower isocyanate content met the standard requirements for automotive seating applications. In fact, using lignin polyols as a replacement for petrochemical polyols also allowed a 5-10% reduction in the amount of isocyanate. This indicates that lignin can be used to partially substitute fossil-fueled based polyols while at the same reducing the isocyanate usage. Flexible foams are one segment of the PUs where lignin has struggled to be used effectively. Using PC to prepare lignin polyols with higher aliphatic OH contents that are more reactive toward isocyanates and in a liquid state enabled us to formulate lignin-based PU flexible foam designed for the largest segment of PUs used in the cars. This is a great step towards helping automotive producers to reach their goals of having more sustainable, biobased materials. Additionally, the principal chemical used to make this polyol, propylene carbonate, is a VOC-exempt sustainable solvent

and oxyalkylation reagent. Undoubtedly, a great deal of work is required to improve the properties of these lignin polyols and foams, but these preliminary results indicated that for the first time that foam with 14 wt.% of the lignin polyol can meet the standard mechanical properties required for automotive seating applications.

4.2 Future Work

The first part of this study showed that DFT modeling can effectively be used to model lignin-PU systems. In the future, a combined computational-experimental studies can be executed to give better insight into the fundamentals of a wide variety of reactions for applied lignin chemistry. For instance, DFT modeling could be applied to reactions of lignin with propylene carbonate to predict which catalysts are most effective for lignin oxyalkylation, aiding further development of the lignin polyol technology. Overall, applying computational chemistry to lignin has the potential to provide new insights into lignin's structure and can better inform chemists and engineers working on lignin-based polymer systems.

In addition, this work identified several issues with the development of liquid lignin polyols. Namely, these were the limited flexibility of the foam and the high amount of unreacted PC in the lignin polyols. Future studies will aim to further reduce the amount of unreacted propylene carbonate in lignin-polyol as it can act as a plasticizer and negatively affect foam performance.. Furthermore, more in-depth characterizations can be carried out on the lignin polyol, such as 2D HSQC NMR and GPC analysis to precisely identify the structure of the lignin polyol, and Mark-Houwink parameter fitting could be used to understand the branching and rheology of the lignin-based polyols. Additionally, this project identified that kraft-softwood lignin polyols resulted in the best-performing flexible PU foams. Still, it was not entirely clear whether it was due to the unique structure of softwood lignin or due to that particular lignin's

high molecular weight. Making foams of the same lignin, but with different molecular weight fractions, could give excellent insight into the properties of the polyols.

One key part of this project was to use propylene carbonate as a “green” oxyalkylation agent for the production of polyurethane foams. However, a more in-depth life cycle assessment should be completed to better understand how the use of lignin and propylene carbonate actually impacts the total emissions and cost of flexible foams and polyols. For instance, the fact that propylene carbonate can be synthesized from bio-based materials and carbon dioxide could significantly reduce the greenhouse gas emissions of this lignin polyol compared to similar technologies. Another aspect that could be investigated would be how differences in density and mechanical properties between lignin based foams affect the total emissions and cost during the end use of the product in automobiles.

Additionally, more advanced characterization techniques can be used to better understand the PU foam morphology. These include transmission electron microscopy, small-angle x-ray scattering, and atomic force microscopy. Knowing precisely how lignin polyol interacts with the hard and soft domains of the polymer matrix would enable a much better understanding of how the lignin polyol affects the mechanical properties of flexible PU foams.

BIBLIOGRAPHY

- (1) Ionescu, M. *Chemistry and Technology of Polyols for Polyurethanes*, 2nd Edition *Chemistry and Technology of Polyols for Polyurethanes*, 2nd Edition; 2016; Vol. 2.
- (2) Szycher's Handbook of Polyurethanes. *Szycher's Handbook of Polyurethanes* **1999**, undefined-undefined. <https://doi.org/10.1201/9781482273984>.
- (3) Flory, P. J. Molecular Theory of Rubber Elasticity. *Polymer (Guildf)* **1979**, 20 (11), 1317–1320. [https://doi.org/10.1016/0032-3861\(79\)90268-4](https://doi.org/10.1016/0032-3861(79)90268-4).
- (4) Gallu, R.; Méchin, F.; Dalmas, F.; Gérard, J. F.; Perrin, R.; Loup, F. On the Use of Solubility Parameters to Investigate Phase Separation-Morphology-Mechanical Behavior Relationships of TPU. *Polymer (Guildf)* **2020**, 207, 122882. <https://doi.org/10.1016/J.POLYMER.2020.122882>.
- (5) Ginzburg, V. V; Bicerano, J.; Christenson, C. P.; Schrock, A. K.; Patashinski, A. Z. Theoretical Modeling of the Relationship between Young's Modulus and Formulation Variables for Segmented Polyurethanes. *J Polym Sci Part B: Polym Phys* **2007**, 45, 2123–2135. <https://doi.org/10.1002/polb.21213>.
- (6) Kaushiva, B. D.; McCartney, S. R.; Rossmly, G. R.; Wilkes, G. L. Surfactant Level Influences on Structure and Properties of Flexible Slabstock Polyurethane Foams. *Polymer (Guildf)* **2000**, 41 (1), 285–310. [https://doi.org/10.1016/S0032-3861\(99\)00135-4](https://doi.org/10.1016/S0032-3861(99)00135-4).
- (7) Current Intelligence Bulletin 51 - Carcinogenic Effects of Exposure to Propylene Oxide. **2020**. <https://doi.org/10.26616/NIOSH PUB89111>.
- (8) Hogstedt, C.; Aringer, L.; Gustavsson, A. Epidemiologic Support for Ethylene Oxide as a Cancer-Causing Agent. *JAMA: The Journal of the American Medical Association* **1986**, 255 (12), 1575–1578. <https://doi.org/10.1001/JAMA.1986.03370120053022>.
- (9) *Polyurethane market value 2030 | Statista*. <https://www-statista-com.proxy2.cl.msu.edu/statistics/720449/global-polyurethane-market-size-forecast/> (accessed 2023-08-15).
- (10) *Polyurethane global market volume 2030 | Statista*. <https://www-statista-com.proxy2.cl.msu.edu/statistics/720341/global-polyurethane-market-size-forecast/> (accessed 2023-08-15).
- (11) Ates, M.; Karadag, S.; Eker, A. A.; Eker, B. Polyurethane Foam Materials and Their Industrial Applications. *Polym Int* **2022**, 71 (10), 1157–1163. <https://doi.org/10.1002/PI.6441>.

- (12) Kaur, R.; Singh, P.; Tanwar, S.; Varshney, G.; Yadav, S. Assessment of Bio-Based Polyurethanes: Perspective on Applications and Bio-Degradation. *Macromol* **2022**, Vol. 2, Pages 284-314 **2022**, 2 (3), 284–314. <https://doi.org/10.3390/MACROMOL2030019>.
- (13) Gadhave, R. V.; Mahanwar, P. A.; Gadekar, P. T.; Gadhave, R. V.; Mahanwar, P. A.; Gadekar, P. T. Bio-Renewable Sources for Synthesis of Eco-Friendly Polyurethane Adhesives—Review. *Open Journal of Polymer Chemistry* **2017**, 7 (4), 57–75. <https://doi.org/10.4236/OJPCHEM.2017.74005>.
- (14) Chen, C.; Gnanou, Y.; Feng, X. Ultra-Productive Upcycling CO₂ into Polycarbonate Polyols via Borinane-Based Bifunctional Organocatalysts. *Macromolecules* **2023**, 56 (3), 892–898. https://doi.org/10.1021/ACS.MACROMOL.2C02243/ASSET/IMAGES/LARGE/MA2C02243_0004.JPEG.
- (15) Cifarelli, A.; Boggioni, L.; Vignali, A.; Tritto, I.; Bertini, F.; Losio, S. Flexible Polyurethane Foams from Epoxidized Vegetable Oils and a Bio-Based Diisocyanate. **2021**. <https://doi.org/10.3390/polym13040612>.
- (16) Gurgel, D.; Bresolin, D.; Sayer, C.; Cardozo Filho, L.; Hermes de Araújo, P. H. Flexible Polyurethane Foams Produced from Industrial Residues and Castor Oil. *Ind Crops Prod* **2021**, 164, 113377. <https://doi.org/10.1016/J.INDCROP.2021.113377>.
- (17) *Green and Bio Polyols Market Size & Growth Insights, 2030*. <https://www.psmarketresearch.com/market-analysis/green-bio-polyols-market> (accessed 2023-10-24).
- (18) Crestini, C.; Lange, H.; Sette, M.; Argyropoulos, D. S. *On the Structure of Softwood Kraft Lignin*; Green Chemistry; Vol. 19.
- (19) Mekonnen, T.; Mussone, P.; Khalil, H.; Bressler, D. Progress in Bio-Based Plastics and Plasticizing Modifications. *J Mater Chem A Mater* **2013**, 1 (43), 13379–13398. <https://doi.org/10.1039/C3TA12555F>.
- (20) Katahira, R.; Elder, T. J.; Beckham, G. T. A Brief Introduction to Lignin Structure. *RSC Energy and Environment Series* **2018**, 2018-January (19), 1–20. <https://doi.org/10.1039/9781788010351-00001>.
- (21) Areej, F.; Mohd Ashadie, K.; Zakiah, S.; Ainun, Z. M. A. Pulping Process for Nonwoody Plants. *Pulping and Papermaking of Nonwood Plant Fibers* **2023**, 17–32. <https://doi.org/10.1016/B978-0-323-91625-7.00007-2>.
- (22) Lora, J. Industrial Commercial Lignins: Sources, Properties and Applications. In *Monomers, polymers and composites from renewable resources*; Elsevier, 2008; pp 225–241.

- (23) Gierer, J. Chemistry of Delignification - Part 1: General Concept and Reactions during Pulping. *Wood Sci Technol* **1985**, *19* (4), 289–312. <https://doi.org/10.1007/BF00350807/METRICS>.
- (24) Gierer, J. Chemistry of Delignification. *Wood Sci Technol* **1985**, *19* (4), 289–312.
- (25) Dessbesell, L.; Paleologou, M.; Leitch, M.; Pulkki, R.; Xu, C. C. Global Lignin Supply Overview and Kraft Lignin Potential as an Alternative for Petroleum-Based Polymers. *Renewable and Sustainable Energy Reviews* **2020**, *123*, 109768.
- (26) Jääskeläinen, A. S.; Sun, Y.; Argyropoulos, D. S.; Tamminen, T.; Hortling, B. The Effect of Isolation Method on the Chemical Structure of Residual Lignin. *Wood Sci Technol* **2003**, *37*, 91–102. <https://doi.org/10.1007/s00226-003-0163-y>.
- (27) de Carvalho, D. M.; Colodette, J. L. Comparative Study of Acid Hydrolysis of Lignin and Polysaccharides in Biomasses. *Bioresources* **2017**, *12* (4), 6907–6923. <https://doi.org/10.15376/BIORES.12.4.6907-6923>.
- (28) Liu, J.; Li, X.; Li, M.; Zheng, Y. Lignin Biorefinery: Lignin Source, Isolation, Characterization, and Bioconversion. *Advances in Bioenergy* **2022**, *7*, 211–270. <https://doi.org/10.1016/BS.AIBE.2022.05.004>.
- (29) Bajwa, D. S.; Pourhashem, G.; Ullah, A. H.; Bajwa, S. G. A Concise Review of Current Lignin Production, Applications, Products and Their Environmental Impact. *Ind Crops Prod* **2019**, *139*, 111526. <https://doi.org/10.1016/J.INDCROP.2019.111526>.
- (30) Haridevan, H.; Evans, D. A. C.; Ragauskas, A. J.; Martin, D. J.; Annamalai, P. K. Valorisation of Technical Lignin in Rigid Polyurethane Foam: A Critical Evaluation on Trends, Guidelines and Future Perspectives. *Green Chemistry* **2021**, *23* (22), 8725–8753. <https://doi.org/10.1039/D1GC02744A>.
- (31) Siahkamari, M.; Emmanuel, S.; Hodge, D. B.; Nejad, M. Lignin-Glyoxal: A Fully Biobased Formaldehyde-Free Wood Adhesive for Interior Engineered Wood Products. **2022**. <https://doi.org/10.1021/acssuschemeng.1c06843>.
- (32) Nikafshar, S.; Wang, J.; Dunne, K.; Sangthonganotai, P.; Nejad, Dr. M.; Nejad, M. Choosing the Right Lignin to Fully Replace Bisphenol A in Epoxy Resin Formulation. *ChemSusChem* **2021**, *14* (4), 1184. <https://doi.org/10.1002/CSSC.202002729>.
- (33) Alinejad, M.; Henry, C.; Nikafshar, S.; Gondaliya, A.; Bagheri, S.; Chen, N.; Singh, S. K.; Hodge, D. B.; Nejad, M. Lignin-Based Polyurethanes: Opportunities for Bio-Based Foams, Elastomers, Coatings and Adhesives. *Polymers (Basel)* **2019**, *11* (7), 1202. <https://doi.org/10.3390/polym11071202>.

- (34) Liu, W.; Fang, C.; Wang, S.; Huang, J.; Qiu, X. High-Performance Lignin-Containing Polyurethane Elastomers with Dynamic Covalent Polymer Networks. **2019**. <https://doi.org/10.1021/acs.macromol.9b01413>.
- (35) Lima García, J.; Pans, G.; Phanopoulos, C. Use of Lignin in Polyurethane-Based Structural Wood Adhesives. *J Adhes* **2018**, *94* (10), 814–828. <https://doi.org/10.1080/00218464.2017.1385458>.
- (36) Liu, J.; Liu, H. F.; Deng, L.; Liao, B.; Guo, Q. X. Improving Aging Resistance and Mechanical Properties of Waterborne Polyurethanes Modified by Lignin Amines. *J Appl Polym Sci* **2013**, *130* (3), 1736–1742. <https://doi.org/10.1002/APP.39267>.
- (37) Manzardo, A.; Marson, A.; Roso, M.; Boaretti, C.; Modesti, M.; Scipioni, A.; Lorenzetti, A. Life Cycle Assessment Framework to Support the Design of Biobased Rigid Polyurethane Foams. *ACS Omega* **2019**, *4* (9), 14114–14123. https://doi.org/10.1021/ACSOMEGA.9B02025/ASSET/IMAGES/MEDIUM/AO9B02025_M003.GIF.
- (38) Moretti, C.; Corona, B.; Hoefnagels, R.; Vural-Gürsel, I.; Gosselink, R.; Junginger, M. Review of Life Cycle Assessments of Lignin and Derived Products: Lessons Learned. *Science of The Total Environment* **2021**, *770*, 144656. <https://doi.org/10.1016/J.SCITOTENV.2020.144656>.
- (39) Henry, C.; Gondaliya, A.; Thies, M.; Nejad, M. Studying the Suitability of Nineteen Lignins as Partial Polyol Replacement in Rigid Polyurethane/Polyisocyanurate Foam. *Molecules* **2022**, *27* (8). <https://doi.org/10.3390/MOLECULES27082535>.
- (40) Henry, C.; Tindall, G.; Thies, M. C.; Nejad, M. Fractionated and Purified Hybrid Poplar Lignins as a Polyol Replacement in Rigid Polyurethane/Polyisocyanurate Foams. *J Appl Polym Sci* **2023**, *140* (45), e54648. <https://doi.org/10.1002/APP.54648>.
- (41) Henry, C.; Tindall, G.; Thies, M. C.; Nejad, M. Fractionated and Purified Hybrid Poplar Lignins as a Polyol Replacement in Rigid Polyurethane/Polyisocyanurate Foams. *J Appl Polym Sci* **2023**, *140* (45), e54648. <https://doi.org/10.1002/APP.54648>.
- (42) Henry, C.; Nejad, M. Lignin-Based Low-Density Rigid Polyurethane/Polyisocyanurate Foams. **2023**. <https://doi.org/10.1021/acs.iecr.2c03728>.
- (43) Jeong, H.; Park, J.; Kim, S.; Lee, J.; Ahn, N. Compressive Viscoelastic Properties of Softwood Kraft Lignin-Based Flexible Polyurethane Foams. *Fibers and Polymers* **2013**, *14* (8), 1301–1310. <https://doi.org/10.1007/S12221-013-1301-2/METRICS>.
- (44) Cinelli, P.; Anguillesi, I.; Lazzeri, A. Green Synthesis of Flexible Polyurethane Foams from Liquefied Lignin. *Eur Polym J* **2013**, *49* (6), 1174–1184. <https://doi.org/10.1016/J.EURPOLYMJ.2013.04.005>.

- (45) Bernardini, J.; Cinelli, P.; Anguillesi, I.; Coltelli, M. B.; Lazzeri, A. Flexible Polyurethane Foams Green Production Employing Lignin or Oxypropylated Lignin. *Eur Polym J* **2015**, *64*, 147–156. <https://doi.org/10.1016/J.EURPOLYMJ.2014.11.039>.
- (46) Bernardini, J.; Anguillesi, I.; Coltelli, M. B.; Cinelli, P.; Lazzeri, A. Optimizing the Lignin Based Synthesis of Flexible Polyurethane Foams Employing Reactive Liquefying Agents. *Polym Int* **2015**, *64* (9), 1235–1244. <https://doi.org/10.1002/PI.4905>.
- (47) Wysocka, K.; Szymona, K.; McDonald, A. G.; Mamiński, M.; Maminski, M. Characterization of Thermal and Mechanical Properties of Lignosulfonate- and Hydrolyzed Lignosulfonate-Based Polyurethane Foams. *Bioresources* **2016**, *11* (3), 7355–7364. <https://doi.org/10.15376/BIORES.11.3.7355-7364>.
- (48) Gómez-Fernández, S.; Ugarte, L.; Calvo-Correas, T.; Peña-Rodríguez, C.; Corcuera, M. A.; Eceiza, A. Properties of Flexible Polyurethane Foams Containing Isocyanate Functionalized Kraft Lignin. *Ind Crops Prod* **2017**, *100*, 51–64. <https://doi.org/10.1016/J.INDCROP.2017.02.005>.
- (49) Gómez-Fernández, S.; Günther, M.; Schartel, B.; Corcuera, M. A.; Eceiza, A. Impact of the Combined Use of Layered Double Hydroxides, Lignin and Phosphorous Polyol on the Fire Behavior of Flexible Polyurethane Foams. *Ind Crops Prod* **2018**, *125*, 346–359. <https://doi.org/10.1016/J.INDCROP.2018.09.018>.
- (50) Wang, S.; Liu, W.; Yang, D.; Qiu, X. Highly Resilient Lignin-Containing Polyurethane Foam. *Ind Eng Chem Res* **2019**, *58* (1), 496–504. https://doi.org/10.1021/ACS.IECR.8B05072/ASSET/IMAGES/LARGE/IE-2018-050727_0010.JPEG.
- (51) Ziegłowski, M.; Trosien, S.; Rohrer, J.; Mehlhase, S.; Weber, S.; Bartels, K.; Siegert, G.; Trellenkamp, T.; Albe, K.; Biesalski, M. Reactivity of Isocyanate-Functionalized Lignins: A Key Factor for the Preparation of Lignin-Based Polyurethanes. *Front Chem* **2019**, *7*, 562.
- (52) Maillard, D.; Osso, E.; Faye, A.; Li, H.; Ton-That, M. T.; Stoeffler, K. Influence of Lignin's PH on Polyurethane Flexible Foam Formation and How to Control It. *J Appl Polym Sci* **2021**, *138* (18), 50319. <https://doi.org/10.1002/app.50319>.
- (53) Gondaliya, A.; Nejad, M. Lignin as a Partial Polyol Replacement in Polyurethane Flexible Foam. *Molecules* **2021**, *Vol. 26, Page 2302* **2021**, *26* (8), 2302. <https://doi.org/10.3390/MOLECULES26082302>.
- (54) Gondaliya, A. M. *COMPARATIVE ANALYSIS OF DIFFERENT LIGNINS AS PARTIAL POLYOL REPLACEMENT IN POLYURETHANE FLEXIBLE FOAM FORMULATIONS*; 2020.

- (55) Ajao, O.; Benali, M.; Faye, A.; Li, H.; Maillard, D.; Ton-That, M. T. Multi-Product Biorefinery System for Wood-Barks Valorization into Tannins Extracts, Lignin-Based Polyurethane Foam and Cellulose-Based Composites: Techno-Economic Evaluation. *Ind Crops Prod* **2021**, *167*, 113435. <https://doi.org/10.1016/J.INDCROP.2021.113435>.
- (56) Quan, P.; Kiziltas, A.; Gondaliya, A.; Siahkamari, M.; Nejad, M.; Xie, X. Kraft Lignin with Improved Homogeneity Recovered Directly from Black Liquor and Its Application in Flexible Polyurethane Foams. *ACS Omega* **2022**. <https://doi.org/10.1021/ACSOMEGA.2C01206>/ASSET/IMAGES/MEDIUM/AO2C01206_M002.GIF.
- (57) Wang, F.; Ma, X.; Wu, J.; Chao, Y.; Xiao, P.; Zhu, J.; Chen, J. Flexible, Recyclable and Sensitive Piezoresistive Sensors Enabled by Lignin Polyurethane-Based Conductive Foam †. *Cite this: Mater. Adv* **2023**, *4*, 586. <https://doi.org/10.1039/d2ma00960a>.
- (58) Wysocka, K.; Szymona, K.; McDonald, A. G.; Mamiński, M. Characterization of Thermal and Mechanical Properties of Lignosulfonate-and Hydrolyzed Lignosulfonate-Based Polyurethane Foams.
- (59) Wang, S.; Liu, W.; Yang, D.; Qiu, X. Highly Resilient Lignin-Containing Polyurethane Foam. *Ind Eng Chem Res* **2019**, *58* (1), 496–504. <https://doi.org/10.1021/ACS.IECR.8B05072>/ASSET/IMAGES/LARGE/IE-2018-050727_0010.JPEG.
- (60) Jeong, J.; Kim, W. S.; Lee, M. W.; Goh, M. Liquefaction of Lignin Using Chemical Decomposition and Its Application to Polyurethane Foam. *ACS Omega* **2021**, *6* (16), 10745–10751. <https://doi.org/10.1021/ACSOMEGA.1C00285>/ASSET/IMAGES/LARGE/AO1C00285_0007.JPEG.
- (61) Alam, D.; Lui, M. Y.; Yuen, A.; Maschmeyer, T.; Haynes, B. S.; Montoya, A. Reaction Analysis of Diaryl Ether Decomposition under Hydrothermal Conditions. *Ind Eng Chem Res* **2018**, *57* (6), 2014–2022. <https://doi.org/10.1021/ACS.IECR.7B04754>/ASSET/IMAGES/LARGE/IE-2017-04754J_0009.JPEG.
- (62) Jensen, M. M.; Djajadi, D. T.; Torri, C.; Rasmussen, H. B.; Madsen, R. B.; Venturini, E.; Vassura, I.; Becker, J.; Iversen, B. B.; Meyer, A. S.; Jørgensen, H.; Fabbri, D.; Glasius, M. Hydrothermal Liquefaction of Enzymatic Hydrolysis Lignin: Biomass Pretreatment Severity Affects Lignin Valorization. *ACS Sustain Chem Eng* **2018**, *6* (5), 5940–5949. <https://doi.org/10.1021/ACSSUSCHEMENG.7B04338>/ASSET/IMAGES/LARGE/SC-2017-04338W_0006.JPEG.
- (63) Laird, D. A.; Brown, R. C.; Amonette, J. E.; Lehmann, J. Review of the Pyrolysis Platform for Coproducing Bio-Oil and Biochar. *Biofuels, Bioproducts and Biorefining* **2009**, *3* (5), 547–562. <https://doi.org/10.1002/BBB.169>.

- (64) Cinelli, P.; Anguillesi, I.; Lazzeri, A. Green Synthesis of Flexible Polyurethane Foams from Liquefied Lignin. *Eur Polym J* **2013**, *49* (6), 1174–1184. <https://doi.org/10.1016/J.EURPOLYMJ.2013.04.005>.
- (65) Wu, L. C. -F; Glasser, W. G. Engineering Plastics from Lignin. I. Synthesis of Hydroxypropyl Lignin. *J Appl Polym Sci* **1984**, *29* (4), 1111–1123. <https://doi.org/10.1002/APP.1984.070290408>.
- (66) Ma, X.; Chen, J.; Zhu, J.; Yan, N.; Ma, X.; Chen, J.; Zhu, J.; Yan, N. Lignin-Based Polyurethane: Recent Advances and Future Perspectives. *Macromol Rapid Commun* **2021**, *42* (3), 2000492. <https://doi.org/10.1002/MARC.202000492>.
- (67) Li, B.; Zhou, M.; Huo, W.; Cai, D.; Qin, P.; Cao, H.; Tan, T. Fractionation and Oxypropylation of Corn-Stover Lignin for the Production of Biobased Rigid Polyurethane Foam. *Ind Crops Prod* **2020**, *143*, 111887. <https://doi.org/10.1016/J.INDCROP.2019.111887>.
- (68) Arbenz, A.; Frache, A.; Cuttica, F.; Avérous, L. Advanced Biobased and Rigid Foams, Based on Urethane-Modified Isocyanurate from Oxypropylated Gambier Tannin Polyol. *Polym Degrad Stab* **2016**, *132*, 62–68. <https://doi.org/10.1016/J.POLYMDEGRADSTAB.2016.03.035>.
- (69) Mahmood, N.; Yuan, Z.; Schmidt, J.; Xu, C. Preparation of Bio-Based Rigid Polyurethane Foam Using Hydrolytically Depolymerized Kraft Lignin via Direct Replacement or Oxypropylation. *Eur Polym J* **2015**, *68*, 1–9. <https://doi.org/10.1016/J.EURPOLYMJ.2015.04.030>.
- (70) Kühnel, I.; Podschun, J.; Saake, B.; Lehnen, R. Synthesis of Lignin Polyols via Oxyalkylation with Propylene Carbonate. *Holzforschung* **2015**, *69* (5), 531–538. <https://doi.org/10.1515/HF-2014-0068/MACHINEREADABLECITATION/RIS>.
- (71) Kühnel, I.; Saake, B.; Lehnen, R. Oxyalkylation of Lignin with Propylene Carbonate: Influence of Reaction Parameters on the Ensuing Bio-Based Polyols. *Ind Crops Prod* **2017**, *101*, 75–83. <https://doi.org/10.1016/j.indcrop.2017.03.002>.
- (72) Lignin-Based Polyurethane Prepolymers, Polymers, Related Compositions, and Related Methods. CA3102994A1, June 14, 2019.
- (73) Pescarmona, P. P. Cyclic Carbonates Synthesised from CO₂: Applications, Challenges and Recent Research Trends. *Curr Opin Green Sustain Chem* **2021**, *29*, 100457. <https://doi.org/10.1016/J.COAGSC.2021.100457>.
- (74) Clements, J. H. Reactive Applications of Cyclic Alkylene Carbonates. *Ind Eng Chem Res* **2003**, *42* (4), 663–674. <https://doi.org/10.1021/IE020678I/ASSET/IMAGES/LARGE/IE020678IF00015.JPEG>.

- (75) Stokes, K.; Mcvenes, R.; Anderson, J. M. Polyurethane Elastomer Biostability. *J Biomater Appl* **1995**, 9 (4), 321–354. <https://doi.org/10.1177/088532829500900402>.
- (76) Rokicki, G.; Kowalczyk, T. Synthesis of Oligocarbonate Diols and Their Characterization by MALDI-TOF Spectrometry.
- (77) Pescarmona, P. P. Cyclic Carbonates Synthesised from CO₂: Applications, Challenges and Recent Research Trends. *Curr Opin Green Sustain Chem* **2021**, 29, 100457. <https://doi.org/10.1016/J.COAGSC.2021.100457>.
- (78) Vieira, F. R.; Barros-Timmons, A.; Evtuguin, D. V.; Pinto, P. C. R. Effect of Different Catalysts on the Oxyalkylation of Eucalyptus Lignoboost® Kraft Lignin. *Holzforschung* **2020**, 74 (6), 567–576. <https://doi.org/10.1515/HF-2019-0274/MACHINEREADEABLECITATION/RIS>.
- (79) Zhang, X.; Kim, Y.; Elsayed, I.; Taylor, M.; Eberhardt, T. L.; Hassan, E. B.; Shmulsky, R. Rigid Polyurethane Foams Containing Lignin Oxyalkylated with Ethylene Carbonate and Polyethylene Glycol. *Ind Crops Prod* **2019**, 141, 111797. <https://doi.org/10.1016/J.INDCROP.2019.111797>.
- (80) Vieira, F. R.; Gama, N. V.; Barros-Timmons, A.; Evtuguin, D. V.; Pinto, P. C. O. R. Development of Rigid Polyurethane Foams Based on Kraft Lignin Polyol Obtained by Oxyalkylation Using Propylene Carbonate. *ChemEngineering* 2022, Vol. 6, Page 95 **2022**, 6 (6), 95. <https://doi.org/10.3390/CHEMENGINEERING6060095>.
- (81) Vieira, F. R.; Barros-Timmons, A.; Evtuguin, D. V.; Pinto, P. C. O. R. Oxyalkylation of Lignoboost™ Kraft Lignin with Propylene Carbonate: Design of Experiments towards Synthesis Optimization. *Materials* **2022**, 15 (5). <https://doi.org/10.3390/MA15051925>.
- (82) Mona Alinejad. A COMPARATIVE STUDY OF LIGNIN REACTIVITY TOWARD ISOCYANATE, Michigan State University, 2022.
- (83) Waleed, H. Q.; Csécsi, M.; Hadjadj, R.; Thangaraj, R.; Pecsmány, D.; Owen, M.; Sz, M.; Ori, "; Fejes, Z.; Viskolcz, B.; Fiser, B. Computational Study of Catalytic Urethane Formation. *Polymers* 2022, Vol. 14, Page 8 **2021**, 14 (1), 8. <https://doi.org/10.3390/POLYM14010008>.
- (84) Zieglowski, M.; Trosien, S.; Rohrer, J.; Mehlhase, S.; Weber, S.; Bartels, K.; Siegert, G.; Trellenkamp, T.; Albe, K.; Biesalski, M. Reactivity of Isocyanate-Functionalized Lignins: A Key Factor for the Preparation of Lignin-Based Polyurethanes. *Front Chem* **2019**, 7, 562. <https://doi.org/10.3389/FCHEM.2019.00562/FULL>.
- (85) Elder, T.; Berstis, L.; Zwirchmayr, N. S.; Beckham, G. T.; Crowley, M. F. The Application of Computational Chemistry to Lignin. *In: Proceedings of the 19th International Symposium on Wood, Fibre and Pulping Chemistry* **2017**, 2017, na. <https://doi.org/10.1021/acssuschemeng.7b01373>.

- (86) Mostaghni, F.; Teimouri, A.; Mirshokraei, S. A. Synthesis, Spectroscopic Characterization and DFT Calculations of β -O-4 Type Lignin Model Compounds. *Spectrochim Acta A Mol Biomol Spectrosc* **2013**, *110*, 430–436. <https://doi.org/10.1016/J.SAA.2013.03.075>.
- (87) Delley, B. An All-electron Numerical Method for Solving the Local Density Functional for Polyatomic Molecules. *J Chem Phys* **1990**, *92* (1), 508–517. <https://doi.org/10.1063/1.458452>.
- (88) Govind, N.; Petersen, M.; Fitzgerald, G.; King-Smith, D.; Andzelm, J. A Generalized Synchronous Transit Method for Transition State Location. [https://doi.org/10.1016/S0927-0256\(03\)00111-3](https://doi.org/10.1016/S0927-0256(03)00111-3).
- (89) Samuilov, A. Y.; Zenitova, L. A.; Levin, Y. A.; Kurdyukov, A. I.; Samuilov, Y. D. The Thermodynamic Parameters of Reactions of Phenyl Isocyanate with Methanol Associates. *Russian Journal of Physical Chemistry A* **2008**, *82* (12), 1999–2004. <https://doi.org/10.1134/S0036024408120042/METRICS>.
- (90) TAPPI, T. 211 Om–93 (1993).“. *Ash in wood, pulp, paper and paperboard: Combustion at 525*.
- (91) Akim, L. G.; Argyropoulos, D. S.; Jouanin, L.; Leplé, J.-C.; Pilate, G.; Pollet, B.; Lapierre, C. Quantitative ³¹P NMR Spectroscopy of Lignins from Transgenic Poplars. *Holzforschung* **2001**, *55* (4), 386–390.
- (92) Argyropoulos, D. S. Quantitative Phosphorus-31 NMR Analysis of Six Soluble Lignins. *Journal of wood chemistry and technology* **1994**, *14* (1), 65–82.
- (93) Meng, X.; Crestini, C.; Ben, H.; Hao, N.; Pu, Y.; Ragauskas, A. J.; Argyropoulos, D. S. Determination of Hydroxyl Groups in Biorefinery Resources via Quantitative ³¹P NMR Spectroscopy. *Nat Protoc* **2019**, *14* (9), 2627–2647.
- (94) Argyropoulos, D. S. Quantitative Phosphorus-31 Nmr Analysis of Lignins, a New Tool for the Lignin Chemist. *Journal of Wood Chemistry and Technology* **1994**, *14* (1), 45–63. <https://doi.org/10.1080/02773819408003085>.
- (95) ASTM International. Standard Practice for Polyurethane Raw Materials: Polyurethane Foam Cup Test. *D7487* **2018**, : *West Con*, 1–5. <https://doi.org/10.1520/D7487-18.2>.
- (96) Flegler, S. L.; Heckman, J. W.; Klomparens, K. L. *Scanning and Transmission Electron Microscopy: An Introduction [Hardcover]*; 1993; Vol. 10.
- (97) Wang, M.-L.; Wang,) M.-L. DFT Study of the Catalytic Mechanism for Urethane Formation in the Presence of Basic Catalyst 1,4-Diazabicyclo[2.2.2]Octane. *Commun. Comput. Chem* **2014**, *2* (1), 23. <https://doi.org/10.4208/cicc.2014.v2.n1.3>.

- (98) Antonino, L. D.; Gouveia, J. R.; de Sousa Júnior, R. R.; Garcia, G. E. S.; Gobbo, L. C.; Tavares, L. B.; Dos Santos, D. J. Reactivity of Aliphatic and Phenolic Hydroxyl Groups in Kraft Lignin towards 4,4' MDI. *Molecules* **2021**, *26* (8).
<https://doi.org/10.3390/MOLECULES26082131>.
- (99) Liu, L. Y.; Cho, M.; Sathitsuksanoh, N.; Chowdhury, S.; Renneckar, S. Uniform Chemical Functionality of Technical Lignin Using Ethylene Carbonate for Hydroxyethylation and Subsequent Greener Esterification. *ACS Sustain Chem Eng* **2018**, *6* (9), 12251–12260.
https://doi.org/10.1021/ACSSUSCHEMENG.8B02649/ASSET/IMAGES/LARGE/SC-2018-02649X_0006.JPEG.
- (100) Gellerstedt, G.; Henriksson, G. Lignins: Major Sources, Structure and Properties. In *Monomers, polymers and composites from renewable resources*; Elsevier, 2008; pp 201–224.
- (101) Fu, J.; Jiang, N.; Ren, D.; Song, Z.; Li, L.; Huo, Z. Hydrothermal Conversion of Ethylene Carbonate to Ethylene Glycol. *Int J Hydrogen Energy* **2016**, *41* (21), 9118–9122.
<https://doi.org/10.1016/J.IJHYDENE.2015.12.083>.
- (102) Szycher, M. *Szycher's Handbook of Polyurethanes*; CRC Press, 1999.
<https://doi.org/10.1201/9781482273984>.
- (103) Kairytė, A.; Vaitkus, S.; Pundienė, I.; Balčiūnas, G. Effect of Propylene Glycol, Rapeseed Glycerine, and Corn Starch Modified Polyol Blends Parameters on the Properties of Thermal Insulating Polyurethane Foams. *Journal of Cellular Plastics* **2019**, *55* (4), 365–384.
https://doi.org/10.1177/0021955X19837507/ASSET/IMAGES/LARGE/10.1177_0021955X19837507-FIG5.JPEG.
- (104) Li, W.; Ryan, A. J.; Meier, I. K. Effect of Chain Extenders on the Morphology Development in Flexible Polyurethane Foam. *Macromolecules* **2002**, *35* (16), 6306–6312.
<https://doi.org/10.1021/MA020231L/ASSET/IMAGES/LARGE/MA020231LF00006.JPG>.
- (105) Dong, D.; Fricke, A. L. Intrinsic Viscosity and the Molecular Weight of Kraft Lignin. *Polymer (Guildf)* **1995**, *36* (10), 2075–2078. [https://doi.org/10.1016/0032-3861\(95\)91455-G](https://doi.org/10.1016/0032-3861(95)91455-G).
- (106) Shchekin, A. K.; Kuchma, A. E.; Aksenova, E. V. The Effects of Viscosity and Capillarity on Nonequilibrium Distribution of Gas Bubbles in Swelling Liquid–Gas Solution. *Colloids and Interfaces 2023, Vol. 7, Page 39* **2023**, *7* (2), 39.
<https://doi.org/10.3390/COLLOIDS7020039>.
- (107) Maiuolo, L.; Olivito, F.; Ponte, F.; Algieri, V.; Tallarida, M. A.; Tursi, A.; Chidichimo, G.; Sicilia, E.; De Nino, A. A Novel Catalytic Two-Step Process for the Preparation of

Rigid Polyurethane Foams: Synthesis, Mechanism and Computational Studies. *React Chem Eng* **2021**, *6* (7), 1238–1245. <https://doi.org/10.1039/D1RE00102G>.

- (108) Kaushiva, B. D. Structure-Property Relationships Of Flexible Polyurethane Foams. **1999**.
- (109) Li, H.; Sun, J.-T.; Wang, C.; Liu, S.; Yuan, D.; Zhou, X.; Tan, J.; Stubbs, L.; He, C. High Modulus, Strength, and Toughness Polyurethane Elastomer Based on Unmodified Lignin. **2017**. <https://doi.org/10.1021/acssuschemeng.7b01481>.
- (110) McClusky, J. V.; Priester, R. D.; O’neill, R. E.; Willkomm, W. R.; Heaney, M. D.; Capel, M. A. The Use of FT-IR and Dynamic SAXS to Provide an Improved Understanding of the Matrix Formation and Viscosity Build of Flexible Polyurethane Foams. *Journal of Cellular Plastics* **1994**, *30* (4), 338–360. https://doi.org/10.1177/0021955X9403000409/ASSET/0021955X9403000409.FP.PNG_V03.
- (111) Choi, T.; Weksler, J.; Padsalgikar, A.; Runt, J. Influence of Soft Segment Composition on Phase-Separated Microstructure of Polydimethylsiloxane-Based Segmented Polyurethane Copolymers. *Polymer (Guildf)* **2009**, *50* (10), 2320–2327. <https://doi.org/10.1016/j.polymer.2009.03.024>.
- (112) *Foam Performance - Polyurethane Foam Association*. <https://www.pfa.org/foam-performance/> (accessed 2023-12-20).
- (113) C.S, L.; T.L, O.; C.H, C.; S, A. Effect of Isocyanate Index on Physical Properties of Flexible Polyurethane Foams. *Malaysian Journal of Science* **2007**, *26* (2), 91–98.
- (114) Vieira, F. R.; Gama, N. V.; Evtuguin, D. V.; Amorim, C. O.; Amaral, V. S.; Pinto, P. C. O. R.; Barros-Timmons, A. Bio-Based Polyurethane Foams from Kraft Lignin with Improved Fire Resistance. *Polymers (Basel)* **2023**, *15* (5). <https://doi.org/10.3390/POLYM15051074/S1>.
- (115) Antonino, L. D.; Gouveia, J. R.; de Sousa Júnior, R. R.; Garcia, G. E. S.; Gobbo, L. C.; Tavares, L. B.; Dos Santos, D. J. Reactivity of Aliphatic and Phenolic Hydroxyl Groups in Kraft Lignin towards 4,4' MDI. *Molecules* **2021**, *26* (8). <https://doi.org/10.3390/MOLECULES26082131>.
- (116) Mathew, A. K.; Abraham, A.; Mallapureddy, K. K.; Sukumaran, R. K. Lignocellulosic Biorefinery Wastes, or Resources? *Waste Biorefinery: Potential and Perspectives* **2018**, 267–297. <https://doi.org/10.1016/B978-0-444-63992-9.00009-4>.

APPENDIX

DMol3 Transition State Search

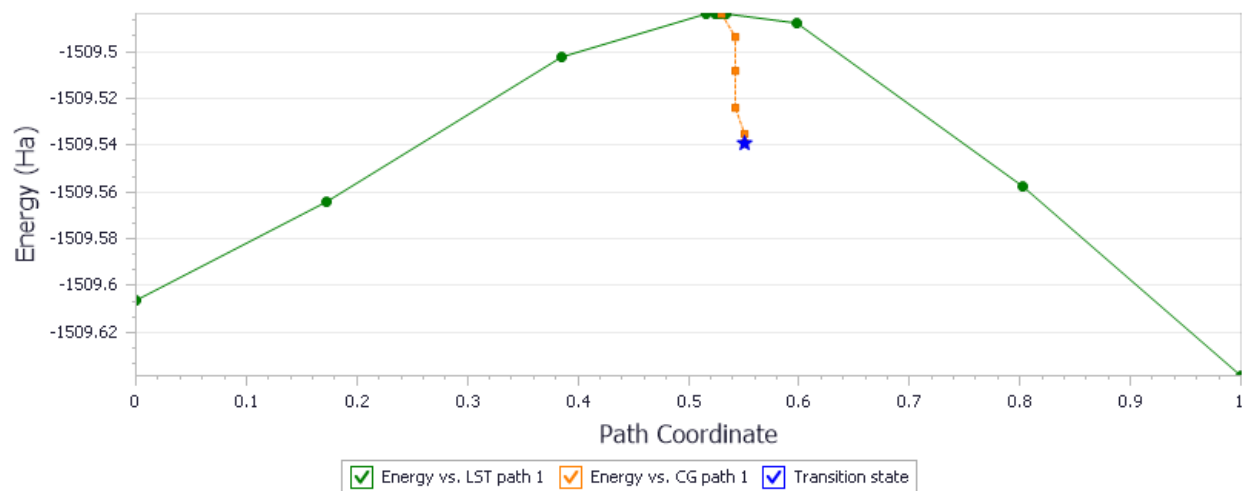


Figure 29. Dmol3 Linear Synchronous Transit Transition State Search, demonstrating how the algorithm first interpolates a reaction pathway, then uses conjugate gradients (CG) to determine the position and energy of the transition state

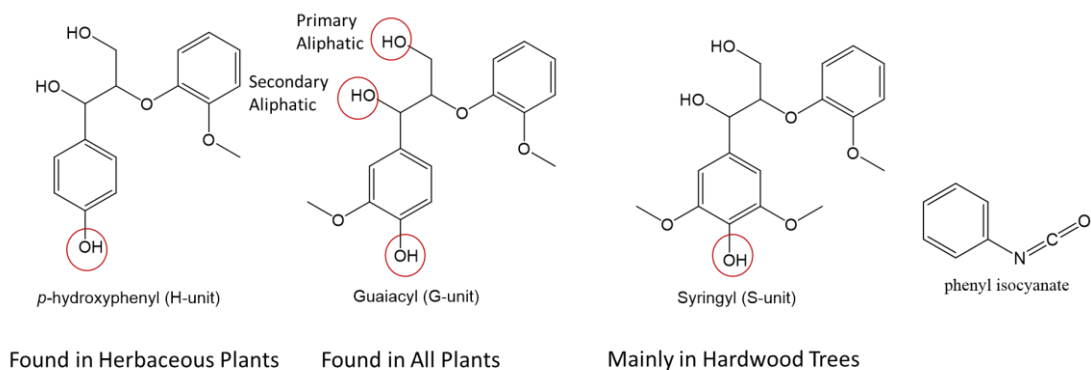


Figure 30. Model compounds used to computationally study lignin-isocyanate reaction

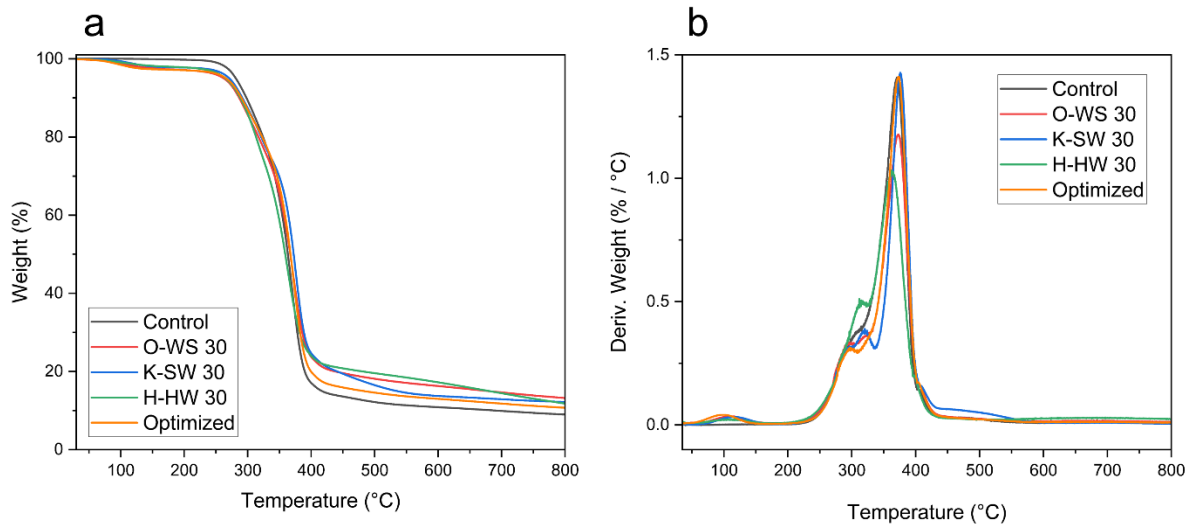


Figure 31. Thermogravimetric analysis of foams made with different lignin polyols, including samples from different lignin polyols

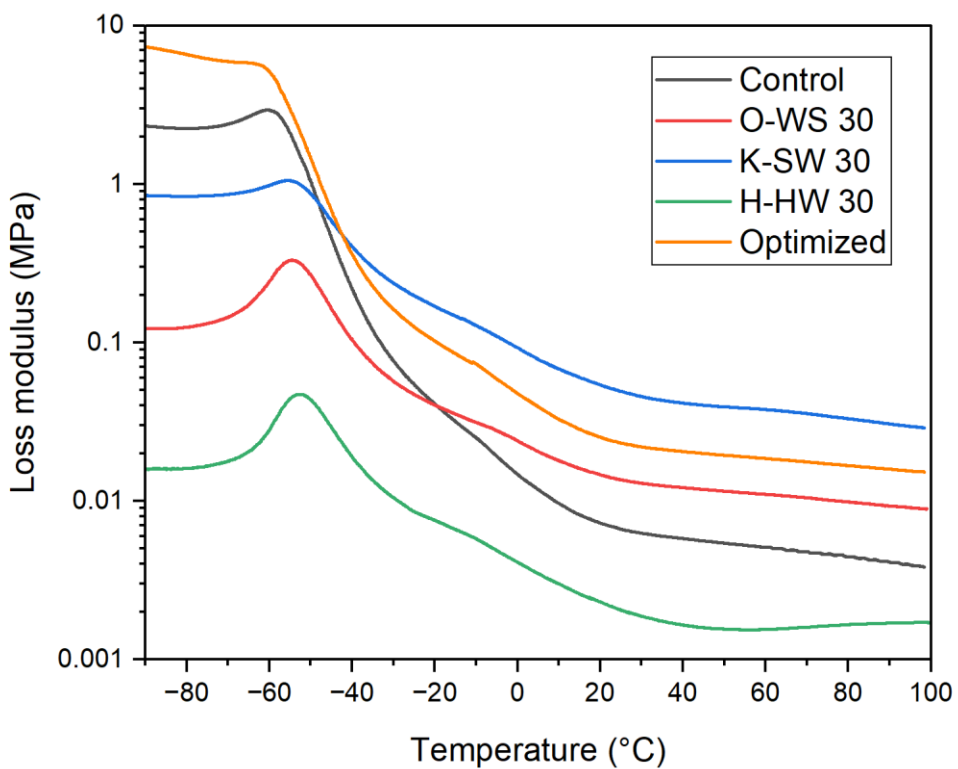


Figure 32. Loss Modulus of Flexible PU Foams with Lignin



Figure 33. 10 lignins and corresponding lignin polyols used during the comparative analysis of lignin polyols

Table 12. Processing parameters for a comparative analysis of eleven lignin polyols

Lignin ID	Sources	Processing	Lignin OH Content (mmol/g)	Lignin (g)	Propylene Carbonate (g)	DBU (g)
1-K-SW	Softwood	Kraft	5.77	50	294	2.20
2-O-SW	Softwood	Organosolv	4.12	50	210	1.57
3-O-HW	Hardwood	Organosolv	4.88	50	249	1.86
4-O-CS	Corn Stover	Organosolv	3.89	50	198	1.48
5-S-WS	Wheat Straw	Soda	5.46	50	278	2.08
6-K-HW	Hardwood	Kraft	5.92	50	302	2.25
7-S-HW	Hardwood	Soda	6.56	50	335	2.50
8-O-WS	Wheat Straw	Organosolv	3.53	50	180	1.34
9-K-HW	Hardwood (Eucalyptus)	Kraft	6.66	50	340	2.53
10-K-SW	Softwood	Kraft	4.66	50	238	1.77
11-O-WS	Wheat Straw	Organosolv	3.73	50	190	1.42

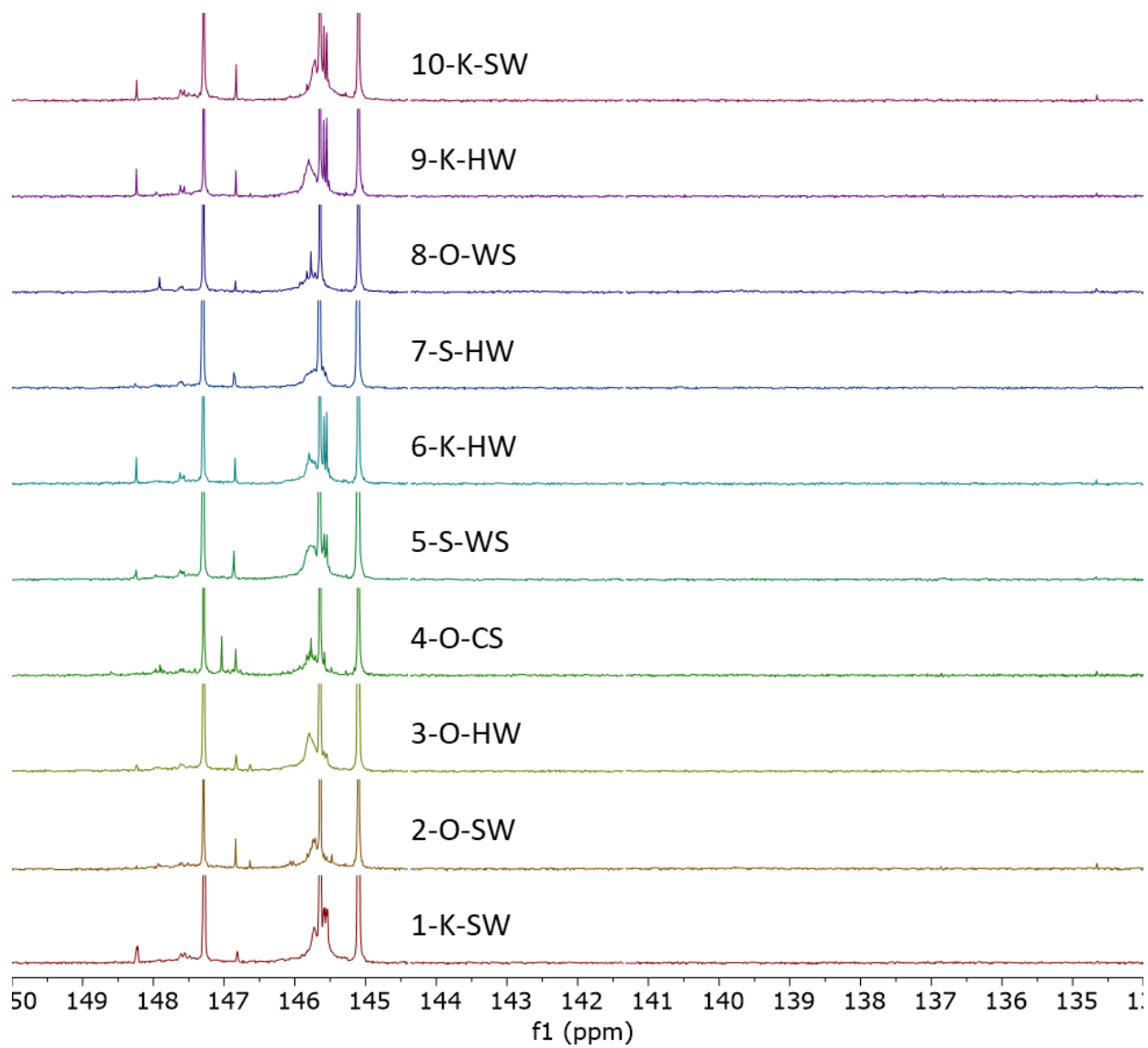


Figure 34. ^{31}P -NMR spectra of samples measured during lignin-polyol comparative analysis

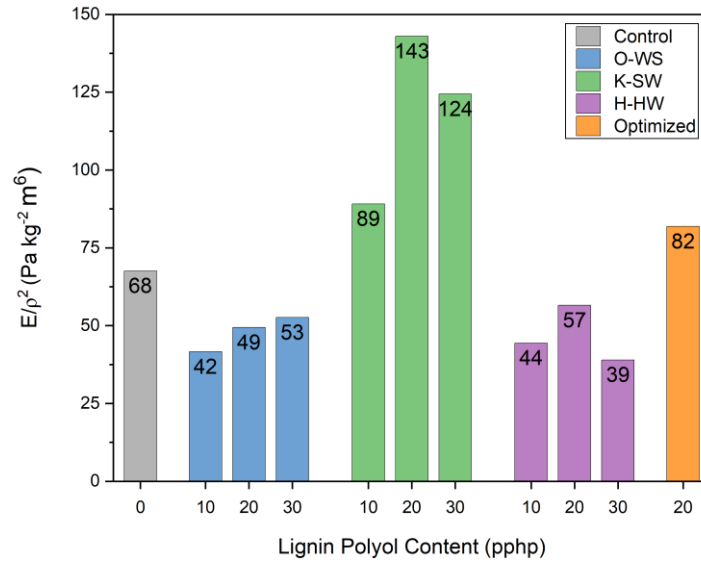


Figure 35. Density-corrected elastic moduli of synthesized PU foams. In theory, foam stiffness is inversely proportional to the square of density, so this represents the actual mechanical properties of the polymer matrix

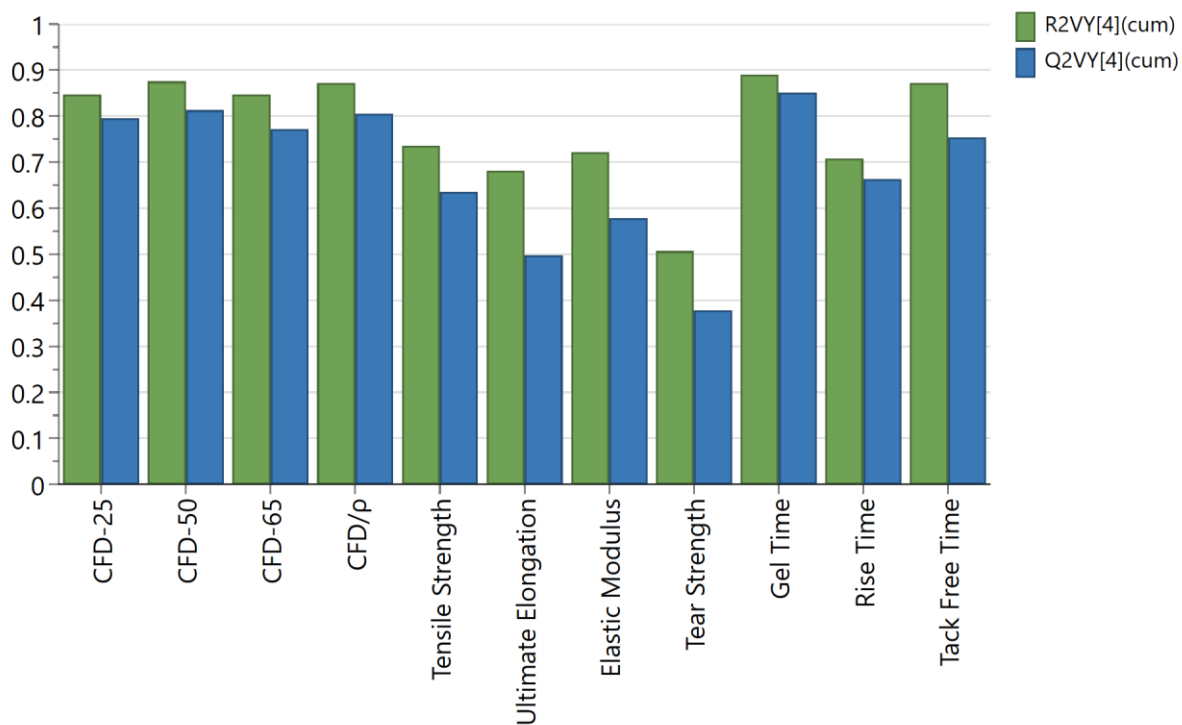


Figure 36. Model accuracy (R2VY) and prediction ability (Q2VY) for a four-component PLS model of flexible PU Foam